Abstract

Pamali, Abhinand P. Using Clothoidal Spirals to Generate Smooth Tool Paths For High Speed Machining. (Under the direction of Dr. Yuan-Shin Lee.)

We present a new and innovative method to generate Contour Parallel tool paths using Clothoidal spirals for 2.5D pocket milling. The tool paths generated by the proposed method are more suitable for High Speed Machining compared to the traditional tool paths. Mechanical parts, such as those in Aerospace industry, Mold and Dies industry, etc require large volumes of milling operations. Modern High Speed CNC Machines are used in making of these parts. Although the High Speed CNC machines can provide very high spindle speed, due to various reasons, it has not been possible to use their High speed capabilities to their full extent. Two of the main reasons being, complex pocket geometry and complex tool path geometry. Most pockets are made up of sharp corners. In the traditional contour parallel pocket milling tool paths, as the cutting tool approaches these corners, they have to undergo a sudden change in directions and the acceleration of the tool has to be instantaneously decreased. Also, there is an instantaneous increase in the chip volume and the resultant forces acting on the cutting tool. In our proposed method we smooth these sharp corners of the traditional tool path by using Clothoidal spirals. The Clothoidal curves which have traditionally been used for Highways and Rail track design, have an unique property, according to which, the curvature of the Clothoidal spirals varies linearly with the length of the curve. By using these curves of uniformly varying curvature, we reduce the magnitude of the sudden direction changes that the cutting tool has to undergo at the sharp pocket corners. The cutting tool is subjected to lesser resultant forces and has a comparatively uniform acceleration. Machining time is also expected to be reduced by our proposed method.

USING CLOTHOIDAL SPIRALS TO GENERATE SMOOTH TOOL PATHS FOR HIGH SPEED MACHINING

By
Abhinand P Pamali

A thesis submitted to the Graduate Faculty of
North Carolina State University
in partial fulfillment of the
requirements for the Degree of
Master of Science

Industrial Engineering

Raleigh
Spring-2004

Approved by:

Dr.Yuan-Shin Lee **Chair of Advisory Committee**	**Dr.Ezat Sanii**
Dr. Robert E. Young	**Dr. Stephen Roberts**

Dedication:

The work represented by this thesis is dedicated to my Parents, Pandurang and Nirmala Pamali, Brother Aravind Pamali, Teachers and Friends.

Biography:

Abhinand Pamali was born in Hubli, India. He received his B.E degree in Mechanical Engineering in 2000 from Karnataka University, Dharwad, India with First Class in Distinction. Abhinand is an active member of IIE and SME and has formerly been an office bearer of SME and many other organizations in his native country. Apart from CAD/CAM, he is also interested in Databases and Economics. His non academic interests include traveling, politics and sports.

Acknowledgments:

I am deeply indebted to Dr. Lee for his inspiration, direction and patience with this project. I would like to express my deep appreciation to Dr. Sanii, Dr. Young and Dr.Roberts not only for serving on my committee but for all my coursework under their direction. I would like to thank Dr.Ajay Joneja for his extremely valuable feedback during the course of our discussions. I would also like to thank Dr. Yau, Dr. Jun and Dr. Ju, Visiting Professors to Dr. Lee's group for their valuable guidance. My special thanks also go to Dr. Kay who agreed to serve on my committee although I requested him in the last moment. I would also like to thank members of the research group: Dr. Jirawan Kloypayan, Dr. Yongfu Ren, Dr. Weihang Zhu, Ms. Susana K. Lai-Yuen, Mr. & Mrs. Ron Aman and Mr. Shiyong Lin for their friendship and invaluable time during all my days in NC State.

Table of Contents

Page

List of Figures……vii

List of Tables……ix

1. Introduction……1

1.1. Pocket Milling……...1

1.2. Organization of Thesis……..4

2. Literature Review……...5

2.1. High Speed Machining……5

2.2. High Speed Machining and Pocket Geometry……..6

2.3. Tool Path Planning……....7

2.4. Summary……...15

3. Clothoidal Spirals and Their Use in Generating Planar Curves……...16

3.1. Introduction to the Problem……..16

3.2. Clothoidal Curves…….....17

3.3. Computation of Fresnel Integrals…….20

3.4. Connecting Two Straight Lines with a Pair of Clothoidal Curves……...23

3.5. Summary…….....26

4. Boundary Parallel Tool Path Generation Using Clothoidal Spirals…….27

4.1. Using Clothoidal Curves for High Speed Tool Machining Tool Path Generation…….27

4.2. Tool Path Generation For Convex Corner……...27

4.3. Tool Path Generation For Concave Corner...……..32

4.4. Proposed Clothoid Curve Tool Path Algorithm…….36

5. Computer Implementation and Examples……40

5.1. Computer Implementation…….40

5.2. Summary……48

6. Conclusion……....49

6.1. Conclusion……49

6.2. Future Work……...50

7. References……....51

List of Figures:

Figure 1-1 Graphical representation of pocket milling operation……...2

Figure 1-2 Mechanical part that has large number of pockets in it……2

Figure 2-1 Example of Zig tool path……..8

Figure 2-2 Example of Zig-Zag tool path…….....8

Figure 2-3 Example of Smoot Zig-Zag tool path.....……9

Figure 2-4 Example of Contour Parallel Tool Path.....……9

Figure 2-5 Example of Spiral Tool Path……10

Figure 2-6 The curvature of line-arc-line tool paths has discontinuities at junction points, while the curvature of Bi-clothoidal splines changes continuously……14

Figure 3-1 Example of a Clothoid curve... .....……19

Figure 3-2 Maximum tangent angle $\phi_{\max}$ and angle between two lines α ……..24

Figure 3-3 Symmetric half Clothoids being used to connect two straight lines…25

Figure 3-4 Smooth corner between two straight lines formed by Clothoidal interpolation……..... 25

Figure 4-1 A pocket with a convex corner.....……28

Figure 4-2 Line-Line tool path at concave corner……28

Figure 4-3 Line-arc-line tool path at concave corner and Line-Bi-Clothoid-Line conversion……..29

Figure 4-4 Gouging due to distant Clothoid start points……31

Figure 4-5 Uncut regions at the Concave Clothoid corners……..32

Figure 4-6 Clothoid start point search on second offset…….....34

Figure 4-7 Curve showing the change in the distance between the Clothoids at the corners……..…….……35

Figure 5-1 A five sided concave polygonal pocket…….…….....41

Figure 5-2 Traditional boundary parallel spiral tool path for concave polygonal pocket.....41

Figure 5-3 Half width cut becoming a full width cut in the corner……...42

Figure 5-4 First offset and Clothoid start points with initial Clothoids.....…...43

Figure 5-5 Changing the scaling factor to connect the Clothoids.....…...44

Figure 5-6 Increasing curvature of the Clothoid as the starting point is moved nearer to the corner of the offsets……..……..46

Figure 5-7 Bi-Clothoids for the second boundary offsets.....…..47

Figure 5-8 The Spiral tool path with smooth corners……...47

Figure 5-9 Another example of spiral tool path with smooth corners .....…..49

List of Tables:

Table 5-1 Table of values to calculate functions of rational approximations….. 22

Chapter 1. INTRODUCTION

Pocket milling represents an important task in machining of mechanical parts, dies and moulds. We propose a new method of generating boundary parallel tool paths for 2.5D high speed pocket milling using Clothoidal Spirals. A Clothoidal Spiral also known as Cornu Spiral or a Clothoid is frequently used in high-way design. The curvature of the Clothoid is proportional to the length of the curve measured from the origin of the curve. In this thesis we provide a method to generate Boundary Parallel Tool Path with smooth Clothoid Corners for High Speed Machining. As a result of this method, it is expected to achieve faster continuous path motion.

1.1 Pocket Milling

Manufacture of various mechanical parts such as aircraft parts, molds and dies, etc involves high intensity 2.5D pocket milling operations. In 2.5D pocket machining, a pocket is excavated by removing layer(s) of material as shown in Figure 1.1. The tool path for a layer of a pocket is line along which the center of the tool –an end mill, travels as its rotating teeth cut the material. Most machining of aerospace parts can be brought of as pocket machining [Bieterman 02]. An aerospace vehicle needs to be smooth, strong and light weight. Pocket machining with the support structure it leaves between pockets, helps achieve these properties. A typical example of the importance and extensiveness of the use of pocket milling operations can be seen in Figure 1.2.

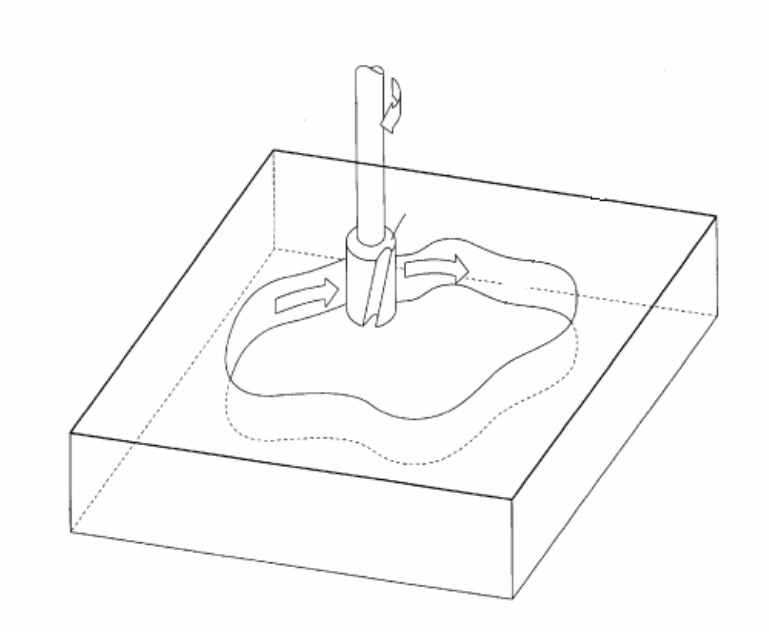

Figure 1.1 Graphical representation of pocket milling operation

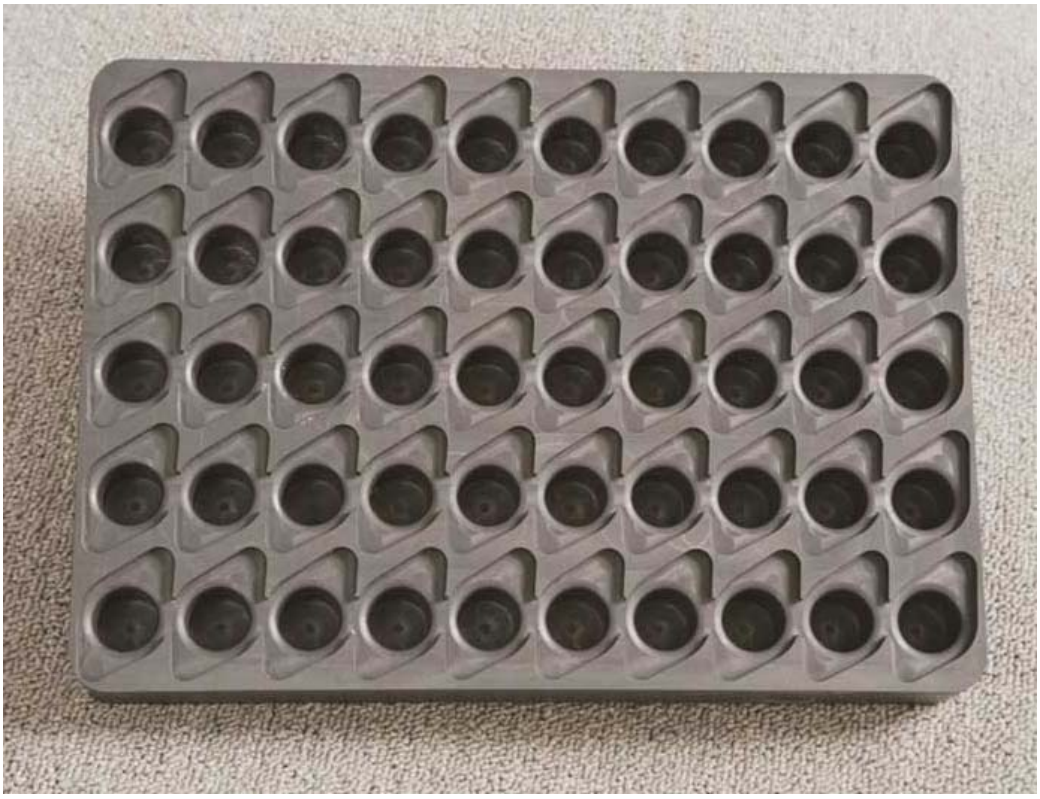

Figure 1.2 Mechanical part that has large number of pockets in it

Due to the large amount of pocket milling needed on many complex mechanical parts, reducing the machining cycle time by even small amounts could bring a significant payback. For the last few years High Speed Machining tools has been vigorously used for large scale pocket milling operations, especially in aerospace and die/mold manufacturing industry.

Although machine tools of very high spindle speeds are available in the market, various machining constraints such as, motion restrictions due to pocket geometry, motion restrictions due to the tool paths, cutting tool strength, effect of the resultant forces on the machine tool, etc keep the users from taking use of the full capabilities of the available High Speed Machine tools.

Tool path generation for pocket milling is mostly done with NC programming, in which a person provides a part description and feed rate requirements to a computer aided manufacturing software package also know as CAM. The CAM package then produces a file with path and feed-rate data that are post processed into a form a controller can understand and use to drive the machine tool. In this thesis, we propose a new method of tool path planning using Clothoidal spirals for smoothening the corners, for pocket milling that will improve upon what the current CAM packages deliver.

1.2 Organization of Thesis

In Chapter 2, a survey of previous work done in high speed machining for pocket milling and tool path generation is provided. Chapter 3 presents the definition and the theory behind the Clothoidal spirals. In Chapter 4, we present the proposed method of smoothing the corners of the boundary parallel offset tool paths and the algorithm used to generate the tool path using the proposed method. In, Chapter 5 shows the computer implementation and some practical examples are discussed. Chapter 6 presents the conclusions and a discussion of future work.

Chapter 2. LITERATURE REVIEW

In this chapter we introduce, previous work done by various researchers in the field of High Speed Machining, Pocket Milling, Tool path planning etc.

2.1 High Speed Machining

High Speed Machining offers a way to mill complex structures that were never practical before. High Speed Machining has enabled users to replace many complex assemblies into a single machined part. Reducing the role of assembly removes cost and lead time from the manufacturing process.

The productivity of a machining operation is often characterized by the metal removal rate. One reason to consider high speed machining applications is to increase productivity without sacrificing part quality. The term 'High Speed Machining (HSM)' is widely accepted and common place in modern machine shops. What is 'High Speed Machining'?

Various sources define High Speed Machining in many different ways. High Speed Machining is a powerful machining method that combines high feed rates with high spindle speeds, specific tools, and specific tool motion. Typically High speed machining uses spindles with high speed and power (generally greater than 10,000 rpm and 10 hp) to remove metal at rates of orders of magnitude higher than by conventional techniques. High Speed Machining addresses part design flexibility, weight savings, part accuracy and part quality, all accomplished while maintaining a high degree of productivity. As briefly indicated earlier in Section 1.1, due to presence of a number of

process constraints in pocket milling the user is discouraged from taking the complete use of the capabilities of the machine tool.

High Speed Machining makes the tool path a more significant factor in the process. Taking lighter cuts with a smaller step-over increment is only one consideration. An effective tool path also protects the cutting tool by keeping cutting load steady and maintains a high feed rate by avoiding sharp changes in direction.

Decisions made during programming can also affect the quality of the work piece. If the purpose of HSM is to machine a smooth surface, the tool path may contribute to this goal. There are a variety of ways to machine with smoother motion. Possibilities include rounding corners, smoothing reversals and even machining in circles.

Another approach to keeping the feed rate high doesn't involve direction changes, but instead involves changing the feed rate more often. Feed rate optimization may allow the program to maintain a higher average feed rate where the profile of the cut frequently changes.

2.2 High Speed Machining and Pocket Geometry

More and more complex mechanical parts that were earlier being assembled or manufactured by other process such as casting etc, are now being machined for various reasons, some of which have been briefly discussed previously. Majority of these parts require lots of pocketing operations. Pocketing operations involve removal of large quantity of material from the metal surface. Due to volume of the machining required for

pocketing operations High Speed Machines are being used for pocket milling of complex parts.

The complexity of the geometry of the pockets greatly reflects on the machining speed that is achieved. Appropriate tool path planning suitable for high speed operations is an important issue in the High Speed Machining Industry. In this report we address this issue of improving the traditional tool paths.

2.3 Tool Path Planning

Two tool path topologies commonly used in milling operations are direction parallel tool path and the contour parallel tool paths, also known as boundary parallel tool paths. The direction parallel tool paths are linear tool paths that can further be classified as, one-way or zig tool path, zig-zag tool path and smooth zig-zag. Figures 2.1, 2.2, and 2.3 show the three different types of direction parallel tool path plans.

The one-way direction parallel tool path system is a uni-directional cutting path, and hence a consistent up-cut or down-cut chip removal can be maintained. However, there is a considerable amount of non-productive time involved in returning the cutter to the start- cut position at the end of each cutting path.

On the other hand, the zig-zag path is a bi-directional cutting path in which material is removed both in the forward and the backward paths. Although the zig-zag tool paths can reduce non-productive tool positioning time, it has a disadvantage that, the

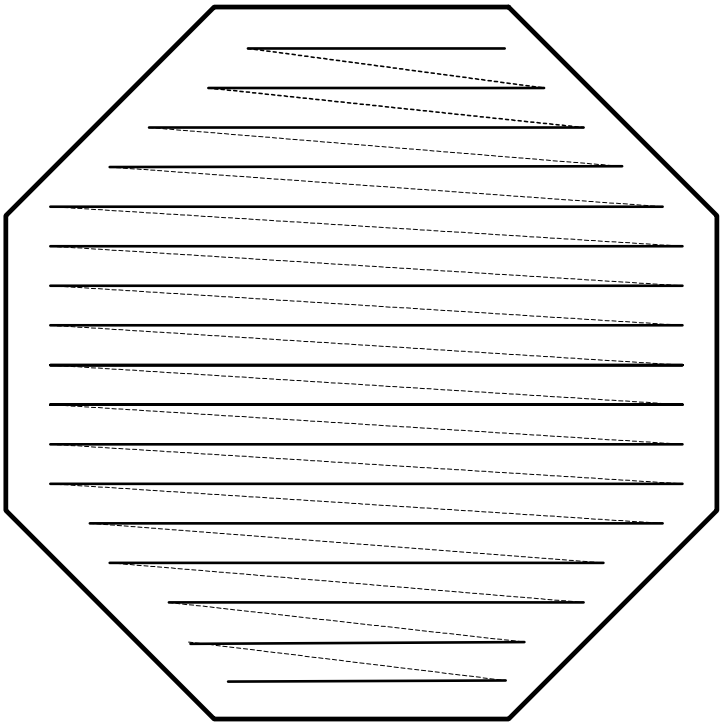

Figure 2.1 Example of Zig tool path

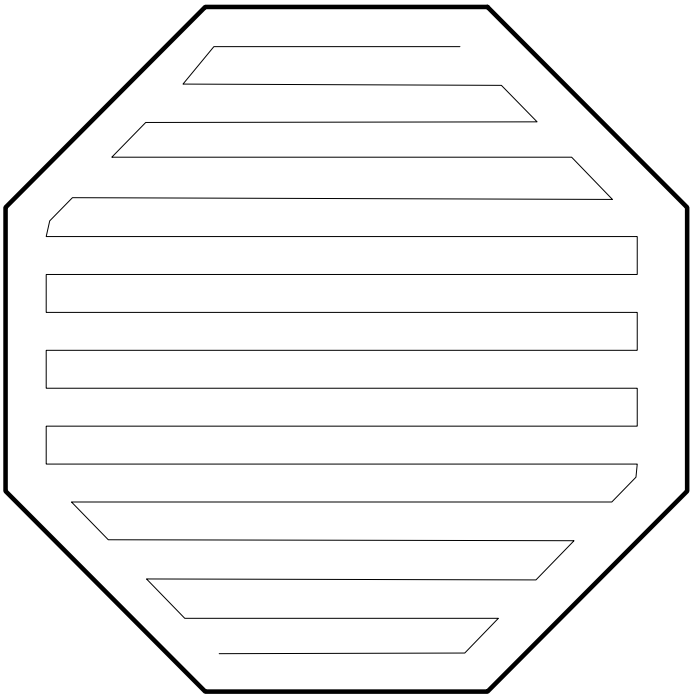

Figure 2.2 Example of Zig-Zag tool path

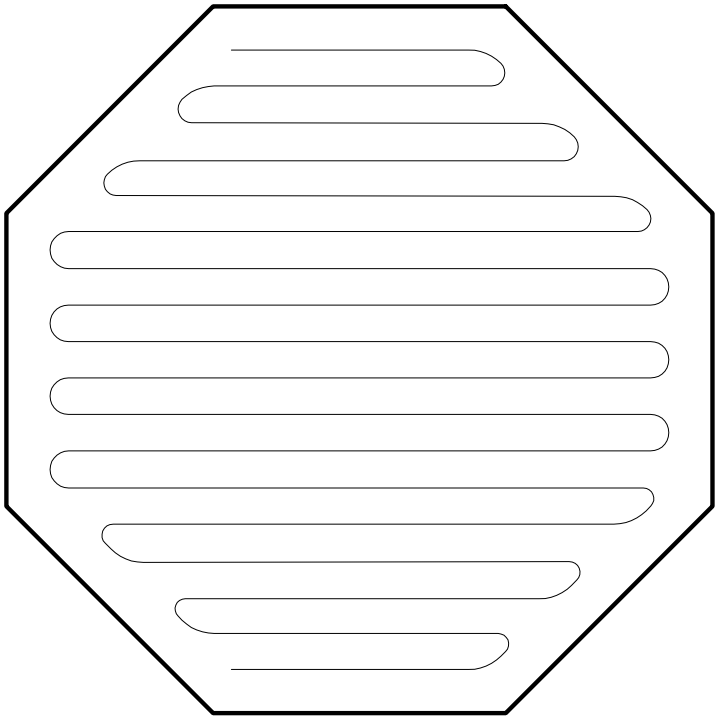

Figure 2.3 Example of Smoot Zig-Zag tool path

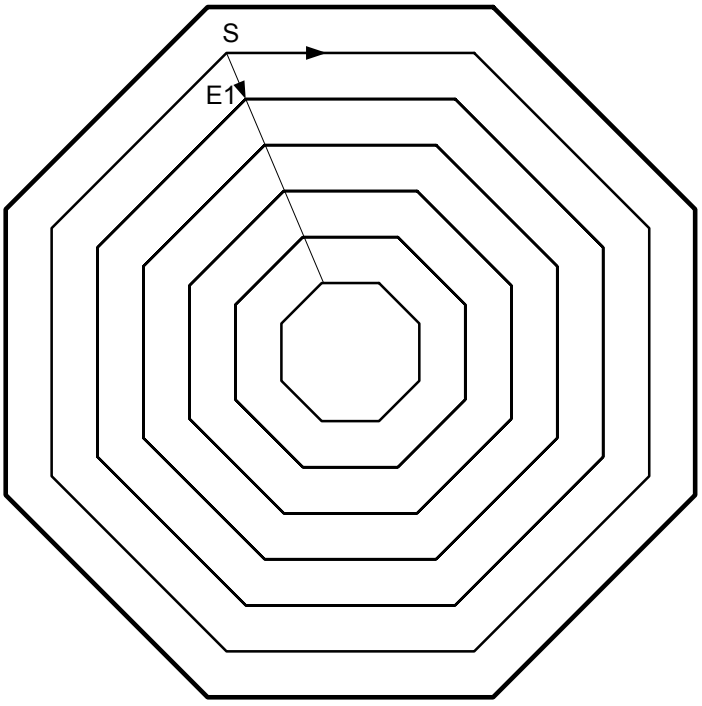

Figure 2.4 Example of Contour Parallel tool path

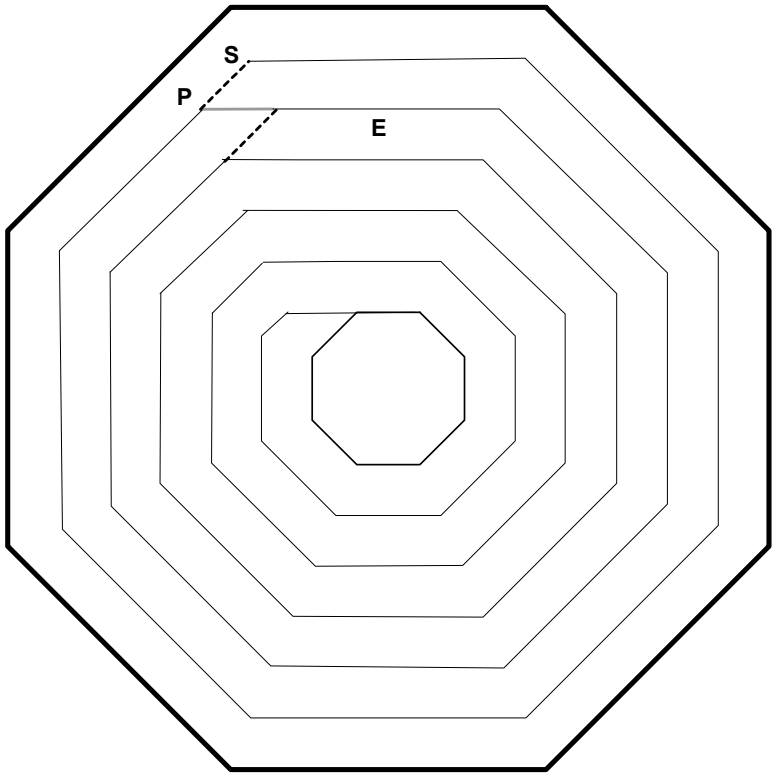

Figure 2.5 Example of Spiral tool path

up-milling and down-milling methods are alternately applied. This will lead to problems such as machine chatter and shorter tool life.

Examples of non-linear tool paths are the contour parallel tool paths and the parametric based tool paths. In contour parallel tool path planning, series of offset contours of the pocket boundary are first generated. The tool travels along these offsets one by one, until the entire pocket is machined. One method of connecting the subsequent contours is shown in Figure 2.4 where the tool begins at the start point, S, goes around the outermost loop, and the moves across the edge marked E1 to reach the next contour. A common variation of this is spiral paths, where the move from one contour to the next contour is computed as follows: the first edge to be machined in the inner loop (edge E in

Figure 2.5), is extended outwards until it intersects the outer loop (at e.g. point P in Figure 2.5). The tool leaves the outer loop at this point P, and moves first along the extension to reach the inner loop.

Parametric based tool path is frequently used as a finishing tool path for machining parametric surfaces as the tool path is driven directly along the u-v parametric curves of the surface itself. As shown in Figure 2.4, contour parallel tool path pattern is derived from the boundary of the concerned machining region. It is a coherent tool in the sense that the cutter is kept in contact with the cutting material most of the time. So it incurs less idle times such as those spent in lifting, positioning and plunging the cutter. At the same time it can also maintain the consistent use of either up-cut or down-cut method throughout the cutting process. Contour-parallel tool path is therefore widely used as a cutting tool path especially for large-scale material removal. A study of machining efficiency comparison of the direction parallel tool paths over the contour parallel tool paths has been done by [Choi 00]. It was found that the smooth zig-zag tool path was most efficient method, closely followed by contour parallel tool path which had sharp corners.

The contour-parallel tool path can be divided into three different approaches: (1) 'pair-wise intersection' [Hansen 92], (2) 'Voronoi Diagram' [Persson 78], (3) 'Pixel-based' [Choi 97]. In the first approach, the boundaries of a machining region are offset inwards by a step over distance. At concave corners the offset segments intersect with each other and hence they need to be trimmed to form the resultant contour profiles. At convex corners, the offset segments are extended and connected to produce the resultant contour profiles. This offsetting, trimming and extending process is repeatedly performed

on each layer of the offset segments until sufficient layers of contour profiles are created for covering the entire machining volume. However eliminating self-interactions is time consuming and the removal of the invalid loops may lead to numerical errors.

In the second approach, individual offset segments are trimmed to their intersections using the Voronoi diagram of the original pocket boundary. This approach is known to be more efficient and robust since the steps in offsetting the tool path segments can be subdivided in a more organized manner. However, as pointed out in [Choi 99], it may also incur numerical instability if it is applied to a boundary of point sequence curve (PS-curve) containing near circular portions.

The third approach of pixel based method requires a large amount of memory and long computation time to achieve a desired level of precision due to its dependence on the resolution of the Z-map.

A new pair-wise offset algorithm based on pair-wise interference detection test was proposed in [Park 01] for removing local invalid loops from the input PS-curve before constructing a raw offset curve. This algorithm has a near O(n) time-complexity, where n is the number of points in the PS-curve. It can avoid the near –circular singularity condition that exists in the traditional pair-wise approach.

No matter which one of the above three approaches is used for tool path generation, concave and convex corners can be found in offset contours by the intersection of the different types of geometric entities such as lines and arcs. The corner-cutting problem provoked by concave and convex corners has not been sufficiently addressed in contemporary CAM systems. For example, many CAM systems will

produce small amount of uncut material at the corner regions when the step over is greater than the cutter.

Also the traditional offsets contours, used directly as tool path have a drawback because when a cutter moves into a corner region, the cutter contact length increases. Consequently, this causes a momentary rise of cutting load, producing undesirable effects such as shorter tool life, machine chatter and even cutter breakage. In a machining process, it is apparent that excessive plunging and slotting, sharp velocity discontinuities, and changing cut geometry limit production rates, increase tool wear, and reduce part quality. To overcome some of these drawbacks, [Chan 01] have proposed a special tool path pattern to machine a concave corner progressively using looping knots. Although the looping knots reduce to some extent, the instant change in acceleration at the corners, the tool path length is increased therefore affecting the efficiency of the process.

Various other researchers have worked on cutting load regularization that is basically classified into (a) online monitoring and control and (b) prediction of cutting loads by cutting load models as an offline approach. Tlusty and Smith (1997) address issues of stability in end milling and the importance of the selecting the proper axial and radial depths of cut for chatter free machining. They avoid over engagement while cornering by adopting a spiral-in approach. Some researchers have used Bezier and B-Spline curves for tool path generation. The Bezier and B-Spline curves are non-linear functions of its parameter, hence an undesirable oscillation may occur [Walton 90].

Walton and Meek (1989) have developed methods to interpolate lines and circular arcs with Clothoidal splines. A Clothoidal curve is unique in the sense that its curvature is a linear function of its parameter.

Use of Clothoidal splines in the pocket corners can therefore reduce the drawbacks such as instantaneous variation in acceleration and feed rate at pocket corners (Figure 2.6).

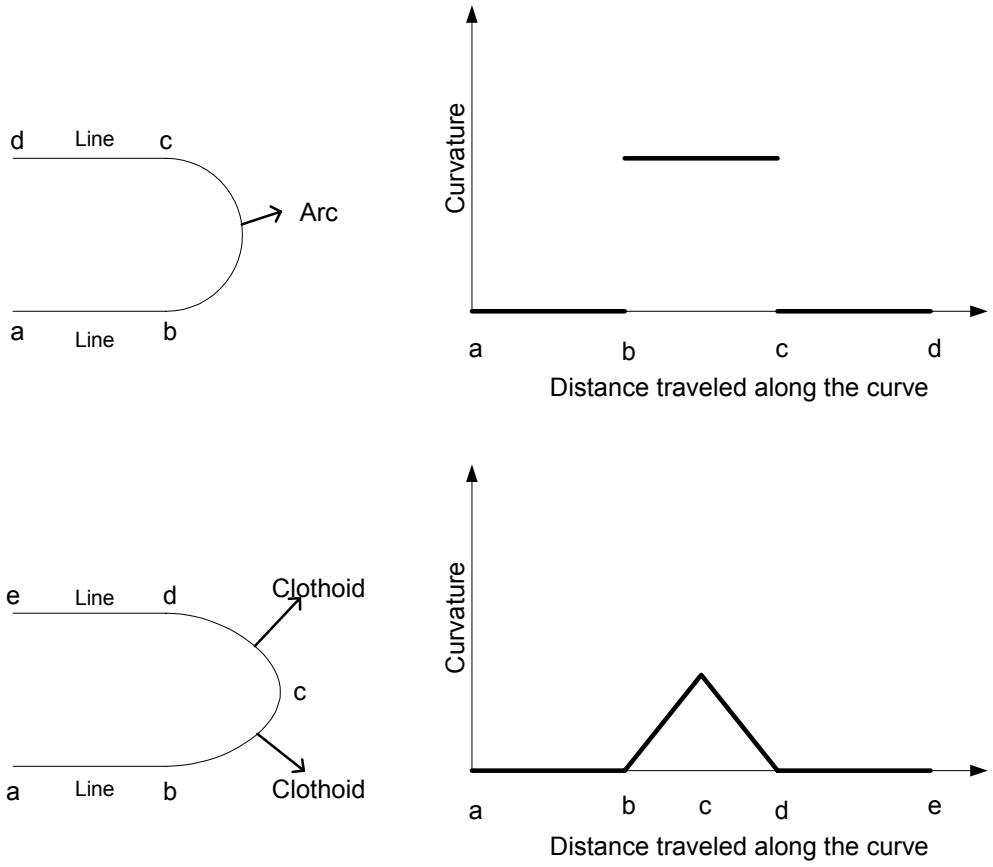

Figure 2.6 The curvature of line-arc-line tool paths has discontinuities at junction points, while the curvature of Bi-clothoidal splines changes continuously

Jirawan (2003), a former member of our group had attempted to use the Clothoidal curves for tool path generation. Jirawan's use of Clothoids in tool path plans showed that Clothoids allow higher feed rates and reduced total machining time. The results of her work involved some uncut regions in the pocket between the contour parallel offsets. To avoid the uncut regions the step distance of the contour offsets was decreased. This resulted in longer tool path, there by affecting its efficiency.

The objective of this thesis is to design optimal contour offset tool path planning using Clothoidal cornering that are guaranteed to avoid undercuts and gouging without reducing the step distance.

2.4 Summary

In this chapter, various traditional tool paths were introduced. We saw that the traditional offsets contours used directly as tool path have various drawbacks, that result in momentary rise of cutting load, producing undesirable effects such as shorter tool life, machine chatter and even cutter breakage. We will discuss our new method to reduce some of these drawbacks in the succeeding chapters.

Chapter 3. CLOTHOIDAL SPIRALS AND THEIR USE IN GENERATING PLANAR CURVES

In this chapter, the Clothoidal curves also known as Cornu spirals are introduced. The mathematical theory behind the Clothoidal curves and the current applications of the Clothoidal curves are discussed. The nature of the Clothoidal curves along with its advantages over other curves is presented. The problem for whose solution we are using the Clothoidal curves is also introduced.

3.1 Introduction to the Problem

High Speed Machining (HSM) involves very high cutting speeds. The cutting tool, the tool stock and the machine tool in general are affected by high forces at the corners while making transition from one geometric shape to another due to the sudden and irregular change in the curvature. This results in increasing wear of the cutting tool/machine tool and hence reducing their life spans and also an inferior surface finish. A reduction in cutting speeds at the corners will result in increased machining time, hence reducing the efficiency.

Traditionally a pair of lines has been cornered by interpolating circular arcs between two sides to obtain a smooth transition between the sides. Circular arc is not sufficient for this problem because at the connecting point with the line there occurs a discontinuous change of curvature. In the next sections of this chapter the Clothoidal Curves, which we have used to get an even smoother transition at the corners are

introduced. A detailed explanation of the nature of the Clothoid curves along with the method to compute them is provided.

3.2 Clothoidal Curves

The Spiral of Cornu is named for the French scientist Marie Alfred Cornu (1841 - 1902). He studied this curve, also known as a Clothoid or Euler's Spiral, in connection with diffraction. Euler applied a similar figure while measuring the elasticity of a spring.

The characteristic property of Clothoid spirals shown in Figure 3.1 is that their curvature is a linear function of the arc length, or in other words the curvature of the curve is proportional to the length of the curve measured from the origin of the spiral. The Clothoid is a planar curve, which is frequently used in highway and railroad designs. A Clothoid is needed to make the gradual transition from a highway, which has zero curvature, to the midpoint of a freeway exit, which has non-zero curvature. A Clothoid is clearly preferable to a path consisting of straight lines and circles, for which the curvature is discontinuous.

The generalization of the Clothoid is given by the following parametric equation as defined in [Gray 97],

$$\text{Clothoid } [n, a](t) = a\left(\int_0^t \sin\left(\frac{u^{n+1}}{n+1}\right)du, \int_0^t \cos\left(\frac{u^{n+1}}{n+1}\right)du\right) \tag{3.1}$$

where n is any positive natural number a and u are scaling factor and parameter, respectively.

The standard Clothoid is defined by Fresnal Integrals invented by Augustine Jean Fresnel (1788-1827) and they are given by,

$$C(u) = \int_0^u Cos \frac{\pi u^2}{2} du \tag{3.2}$$

$$S(u) = \int_0^u Sin \frac{\pi u^2}{2} du \tag{3.3}$$

where *u* is a non-negative parameter. Plotting *C (u)* on the abscissa axis and *S (u)* on the ordinate axis a planar Clothoid curve can be obtained as shown in Figure 3.1.

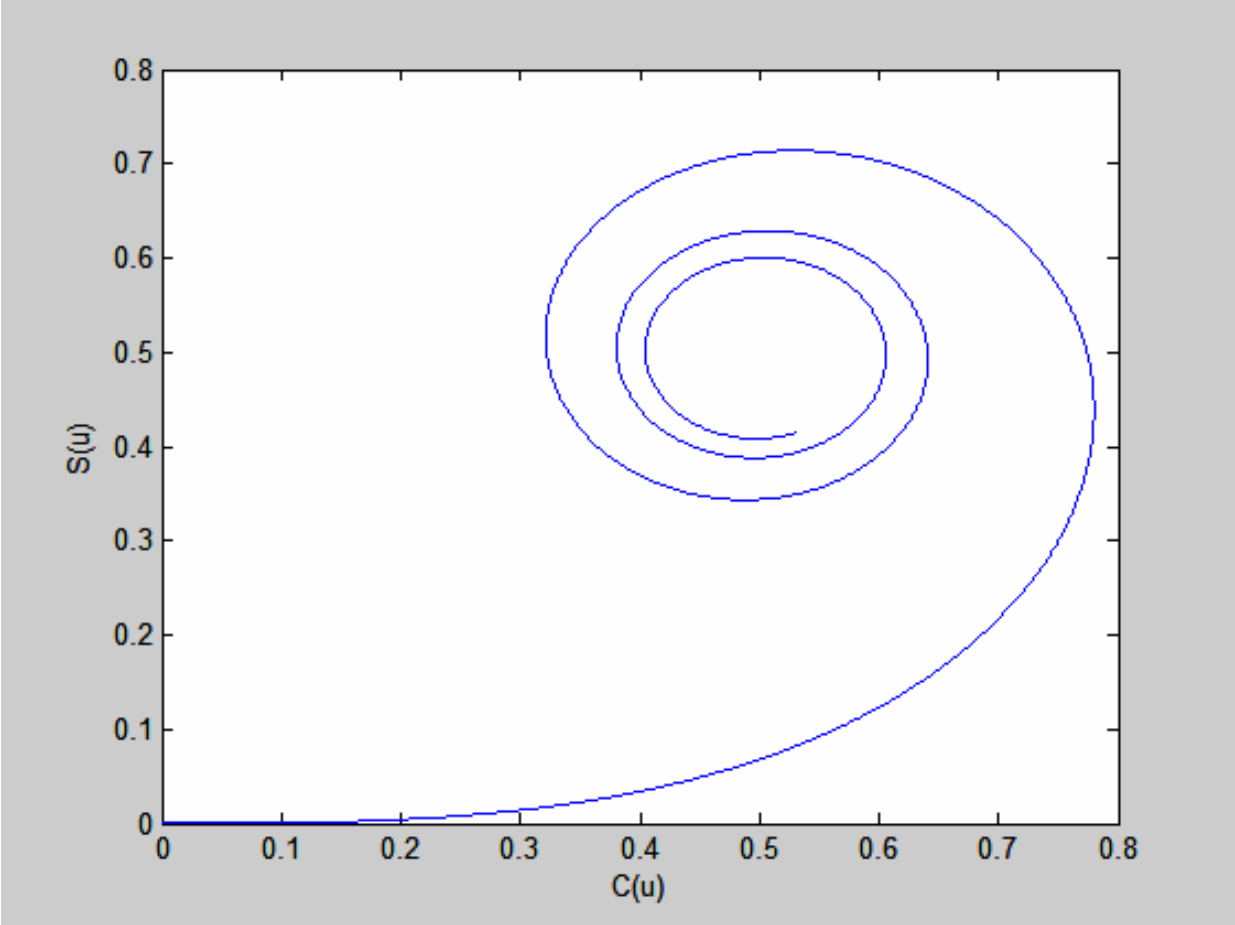

Fig 3.1 Example of a Clothoid curve

3.3 Computation of Fresnal Integrals

The Fresenal Integrals shown in equations (3.2 and (3.3) cannot be solved analytically. We therefore use numerical methods to solve them. Various researchers have proposed numerical methods to approximate the Fresnal integrals. Some of the well known ones being from [Boersma 60, Cody 68, Hastings, Jr 56, Mielenz 97]. In this report we use the Rational Approximations method proposed by [Heald 85] which can approximate the Fresnel Integrals with maximum errors between 1.7×10^{-3} and 4×10^{-8}. The Fresnel Integrals are recast into the polar form shown below,

$$C(u) = \frac{1}{2} - R_{lm}(x)\sin[\frac{1}{2}\pi(A_{jk}(x) - x^2)] \tag{3.4}$$

$$S(u) = \frac{1}{2} - R_{lm}(x)\cos[\frac{1}{2}\pi(A_{jk}(x) - x^2)] \tag{3.5}$$

where the R_{lm} and A_{jk} functions are rational approximations of the form,

$$R_{lm} = \frac{\sum_{i=0}^{l} c_i u^i}{\sum_{i=0}^{m} d_i u^i} \tag{3.6}$$

$$A_{jk} = \frac{\sum_{i=0}^{j} a_i\ u^i}{\sum_{i=0}^{k} b_i u^i} \tag{3.7}$$

The values for $a_{i,}$ $b_{i,}$ c_i and d_i are taken from Table 1 [Heald 85]

An index of orthogonal error in the plane of Cornu spiral which is the diagonal distance between approximated and exact points is given by,

$$\varepsilon = \left[(\delta R)^2 + (\delta A)^2 \right]^{\frac{1}{2}} \tag{3.8}$$

where,

$$\delta R = R_{lm} - R_0 \tag{3.9}$$

$$\delta A = \frac{1}{2} \pi R_0 \left(A_{jk} - A_0 \right) \tag{3.10}$$

The maximum errors within the range of 1.7×10^{-3} and 4×10^{-8} have been show in Table 3.1 from [Heald 85]

R		A		$\varepsilon_{\max}$
$c_0=1$	$d_0=\sqrt{2}$	$a_0=1$	$b_0=2$	
$c_1=0.506$	$d_1=2.054$ $d_2=1.79$		$b_1=2.524$ $b_2=1.886$ $b_3=0.803$	1.7×10^{-3}
$c_1=0.5083$ $c_2=0.3569$	$d_1=2.1416$ $d_2=1.8515$ $d_3=1.11021$	$a_1=0.1765$	$b_1=2.915$ $b_2=2.079$ $b_3=1.519$	1.5×10^{-4}
$c_1=0.60427$ $c_2=0.41159$ $c_3=0.1917$	$d_1=2.26794$ $d_2=2.15594$ $d_3=1.26057$ $d_4=0.60353$	$a_1=0.08218$ $a_2=0.15108$	$b_1=2.7097$ $b_2=2.3185$ $b_3=1.2389$ $b_4=0.6561$	9×10^{-6}
$c_1=0.698773$ $c_2=0.537836$ $c_3=0.246758$ $c_4=0.09458$	$d_1=2.40251$ $d_2=2.45425$ $d_3=1.647924$ $d_4=0.77829$ $d_5=0.297058$	$a_1=0.1446$ $a_2=0.17182$ $a_3=0.056405$	$b_1=2.83577$ $b_2=2.498595$ $b_3=1.61391$ $b_4=0.69638$ $b_5=0.28781$	6×10^{-7}
$c_1=0.7769507$ $c_2=0.6460117$ $c_3=0.3460509$ $c_4=0.1339259$ $c_5=0.0433995$	$d_1=2.5129806$ $d_2=2.7196741$ $d_3=1.9840524$ $d_4=1.0917325$ $d_5=0.4205217$ $d_6=0.13634704$	$a_1=0.1945161$ $a_2=0.2363641$ $a_3=0.068324$ $a_4=0.0241212$	$b_1=2.9355041$ $b_2=2.7570246$ $b_3=1.875721$ $b_4=0.978113$ $b_5=0.356681$ $b_6=0.118247$	4×10^{-8}

Table 3.1 Table of values to calculate functions of rational approximations

[Heald, 85]

3.4 Connecting Two Straight Lines with a Pair of Clothoidal Curves

To connect two directed straight lines, a pair of symmetrical Clothoid curves is used [Walton 89, Makino 88]. Given two lines making an angle α in between them, a pair of symmetric Clothoids with equal scaling parameters is used to plot a corner making a smooth transition from the end point of the first line to the beginning point of the second line. The two Clothoidal curves start from the end point and the beginning point of the first and second straight lines respectively. The curves join the lines at a minimum parameter value u= 0 i.e. the straight line and the Clothoid have the same curvature equal to zero at the point where they meet each other. Let $u_{\max}$ be the value of the parameter at which the two spirals meet i.e. at the point where the curvatures of the two symmetrical Clothoids are maximum and equal.

$u_{\max}$ can be calculated using the Equations (3.11) and (3.12) shown below.

$$\phi_{\max} = \frac{\beta}{2} \tag{3.11}$$

where $\phi_{\max}$ shown in Figure 3.2 is the maximum tangent angle of the Clothoid at the point of intersection of the pair of Clothoids. β, also shown in Figure 3.2 is the maximum tangent angle made by the complete curve (combination of both the symmetrical Clothoids).

$$u_{\max} = \sqrt{\frac{\phi_{\max}}{90}} \tag{3.12}$$

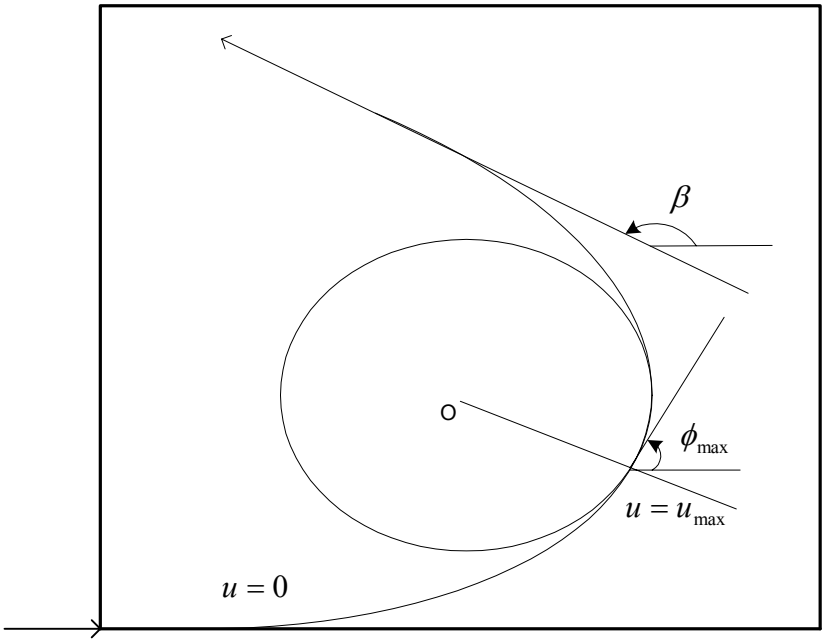

Fig 3.2 Maximum tangent angle ϕ_{max} and angle between two lines α

An example of two straight lines connecting using a pair of symmetric Clothoid curves is shown in Figure 3.3 and Figure 3.4. Figure 3.3 shows a pair of Clothoids emerging from two lines making an angle α between them. The scaling factor in this case is 1. The increase in the scaling factor results in the increase of the size of the Clothoidal Curve. By applying the right scaling factor the pair of the half Clothoids can be connected as shown in Figure 3.4.

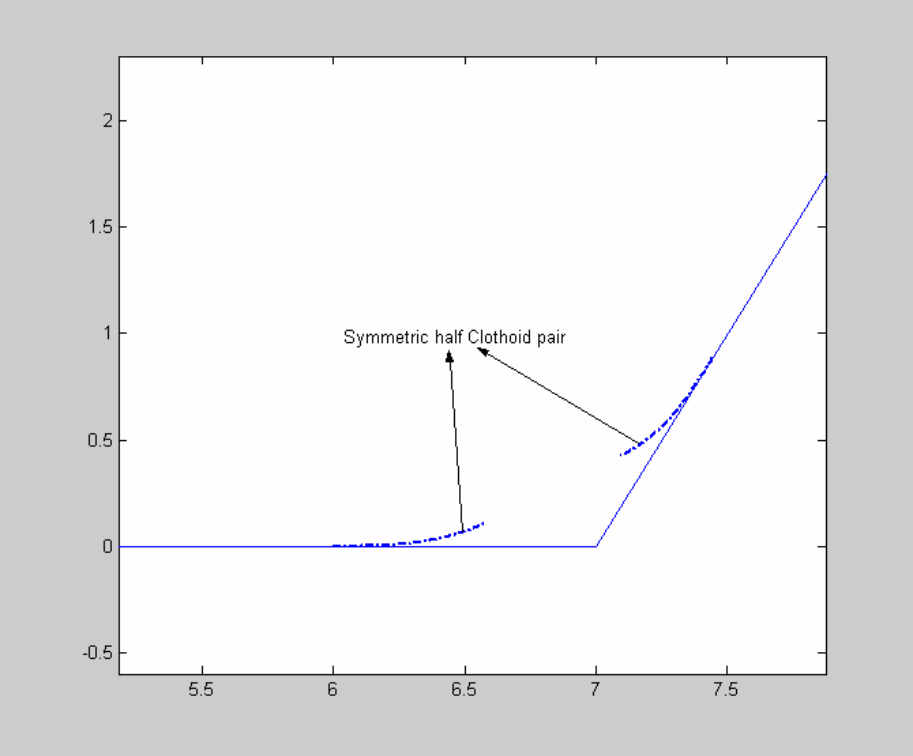

Figure 3.3 Symmetric half Clothoids being used to connect two straight lines.

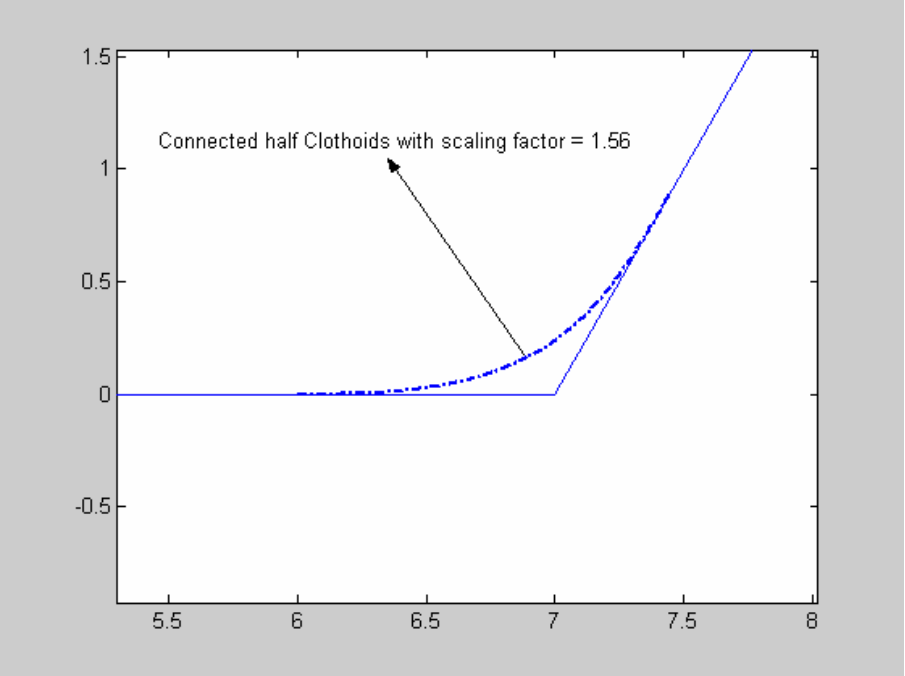

Figure 3.4 Smooth corner between two straight lines formed by Clothoidal interpolation

3.5 Summary

In this chapter the Clothoidal spirals were introduced. The method of generating Clothoidal spirals was discussed. The definitions of Clothoidal spirals cannot be solved numerically. Therefore a simple numerical method known as rational approximation method that is proposed to solve the equations defining the Clothoidal spirals was discussed. The application of these Clothoidal curves in contour parallel tool path generation will be discussed in the next chapter.

Chapter 4. BOUNDARY PARALLEL OFFSET TOOL PATH GENERATION USING CLOTHOIDAL SPIRALS

The goal of this research is to use Bi-Clothoid curves to join boundary parallel offset lines of polygonal pockets to ensure that the tool path generated has a continuous curvature function over the entire cutting plan and the generated tool path does not leave any uncut regions in between adjacent tool path offsets. Detailed procedure and algorithm are presented in this chapter.

4.1 Using Clothoid Curves for High Speed Tool Machining Tool Path Generation

For the purpose of this discussion, we shall always assume that the Clothoid curve undergoes a maximum angle of $\pi/2$. Further, in each case, the objective is to replace a tool path sequences as per the schedule below:

Line-Line → Line- Bi-Clothoid – Line [Figure 4.2a]

Line-Arc-Line → Line – Bi-Clothoid – Line [Figure 4.2b]

In order to use these Splines, we consider two cases: Pocket corners of Concave and Convex shapes. Details are discussed in the following sub-sections.

4.2 Tool Path Generation for Convex Corner

For a convex corner shown in Figure 4.1 the traditional tool path plans use circular arc connectors between the boundary parallel offset lines to guarantee that the tool path is C^1 continuous. In this work we replace the circular arc by a pair of symmetric Clothoids. Figures 4.2 and 4.3 show the two possible traditional tool paths at a concave corner.

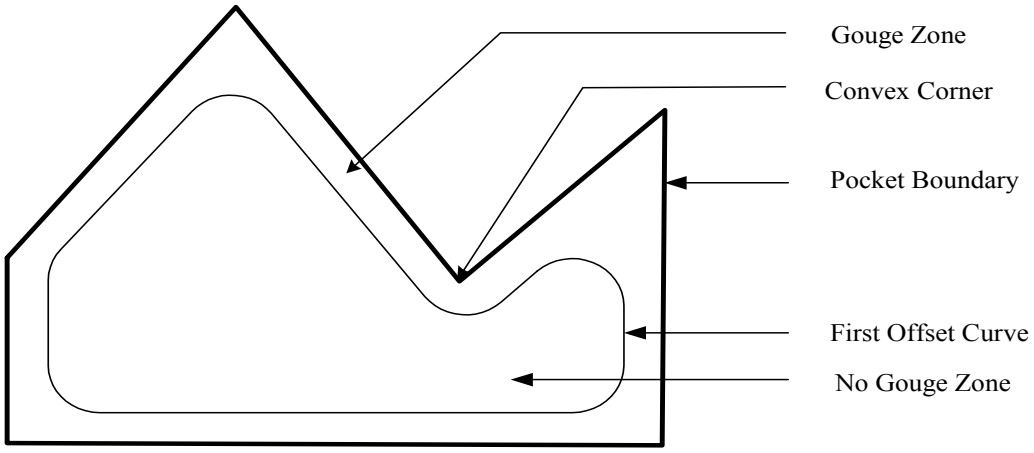

Figure 4.1 A pocket with a convex corner

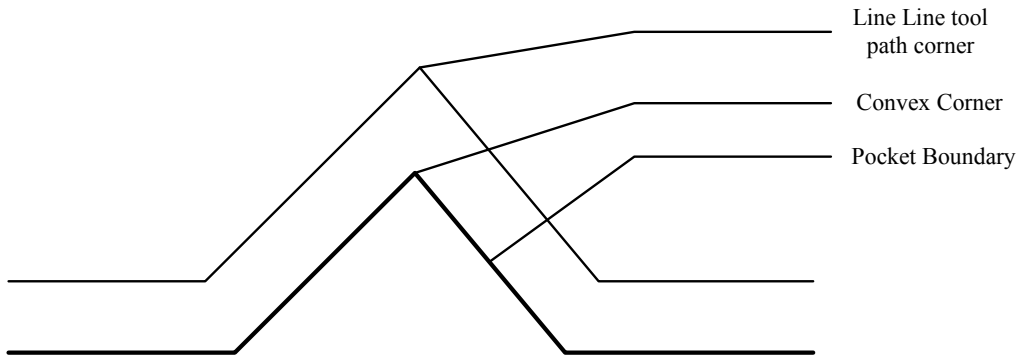

Figure 4.2 Line-Line tool path at convex corner

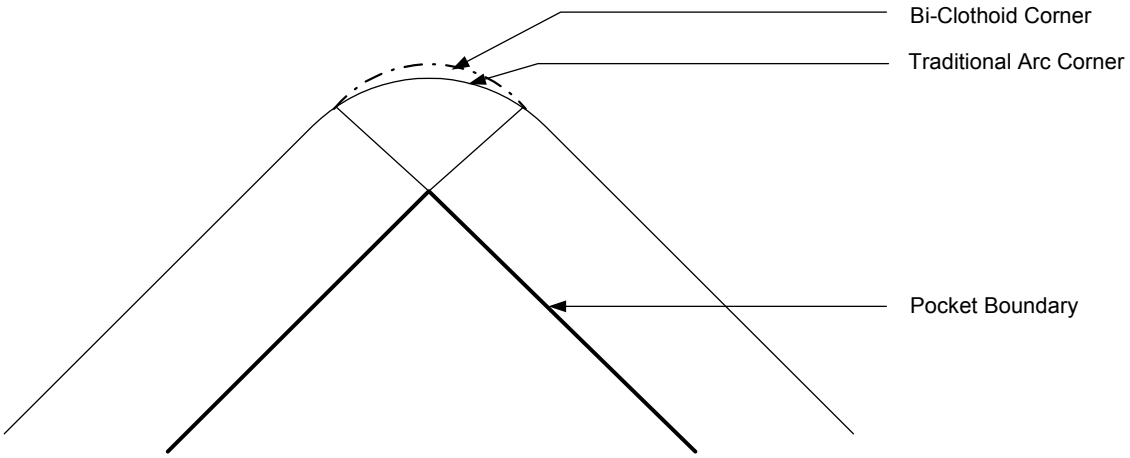

Figure 4.3 Line-arc-line tool path at convex corner and Line-Bi-Clothoid-Line conversion

4.2.1 *Lemma 1.*

Replacing a Line-Line or a Line-arc-Line type of tool path at a convex corner with a Bi-Clothoidal path will result in neither gouging, nor undercuts.

We consider the line-arc-line case. Certainly, the Clothoid cannot begin at a point earlier than the end point of the line segment in the traditional plan. This is because moving an infinitesimal amount along the Clothoid will result in a tool movement towards the pocket boundary (since the clothoid has finite curvature at this point), and therefore the pocket will get gouged.

4.2.2 *Observation 1.*

A Bi-Clothoid(a pair of symmetrical Clothoids) constructed as described earlier ([Chapter 3]), and starting precisely where the circular arc begins does not intersect the circular arc. It is easy to see that initially, the clothoid has curvature smaller than that of the interpolating circular arc, and hence travels to the interior of the pocket, away from the circular arc as shown in Figure 4.3.

The curvature, c_v, of the clothoid is given by

$$c_v = \frac{\pi u}{a} \tag{4.1}$$

where a is the scaling factor and u is the parameter.

Since a is computed numerically for different values of tool radius, R, and included angle, α, therefore one can plot 'safe' regions (values of R and α) for which we can replace precisely the circular arc with a bi-clothoid without any gouging.

For an unsafe combination of R and α, the Clothoid intersects with the circular arc resulting in gouging. This is shown in the Figure 4.4. In such a case, we need to continue along the straight line a little further, before we embark upon the clothoid. i.e. the starting points of the Clothoid are to be taken closer to the corner to obtain a gouge safe path.

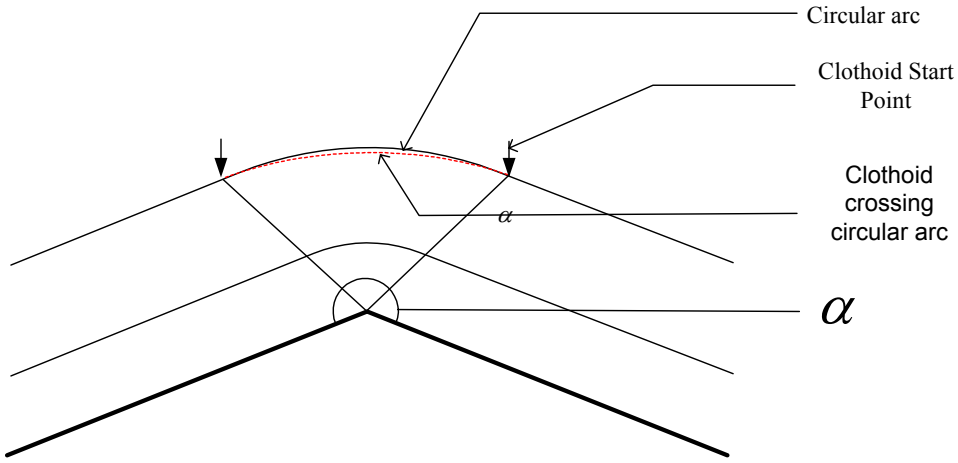

Figure 4.4 Gouging due to distant Clothoid start points.

4.2.2 *Observation 2.*

Since the convex pocket corner is machined precisely by the offset lines, thus in both the above possibilities, there will be no undercut at a convex corner.

The proof of this observation is trivial.

4.3 Tool path generation for Concave corner

We now focus our analysis to concave corners. In this case, due to the geometry, it is possible that the designed Clothoids may leave some un-cut material in the interior of the pocket as shown in Figure 4.5 (Second uncut region). Such un-cut regions are obviously undesirable.

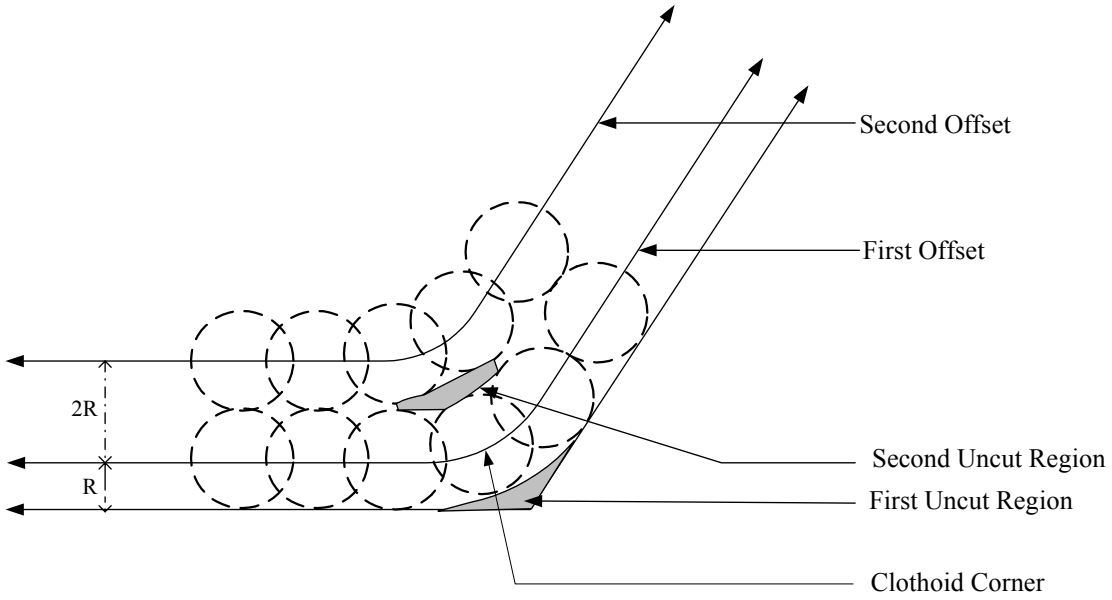

Fig 4.5 Uncut regions at the Concave Clothoid corners

In this section, we shall concentrate on the proper selection of Bi-Clothoids that can avoid such uncut regions. There are two ways to solve this problem.

One way is that, we can reduce the offset distance until there is no remaining uncut area. However, this approach will result in (possibly) more number of offsets and therefore increase the resulting tool-path's length and machining time. We therefore concentrate on the other way which involves selecting a proper Clothoid for the corners that can avoid uncut areas.

It is clear that in any scheme, there is some area at the pocket boundary corners as shown in Figure 4.5 (First uncut region) due to the cylindrical shape of tool. This is usually removed by the finishing operations. Our goal is to ensure that the subsequent uncut areas are completely eliminated.

To analyze this we shall distinguish between the first offset and the subsequent offsets.

4.3.1 *First offset curve*

The only decisions are the selection of the start point of the Clothoid, and, subsequently, the determination of the scaling factor. The start point is user defined based on the tool size and the machine tool capabilities. The amount of leftover material (first uncut region) at the pocket corners that will be removed in the finishing operation shown in Figure 4.5 is also taken into consideration while deciding the start points for the Clothoids of the first boundary offset.

4.3.2 *Subsequent Offset Curve*

Let A and A' be the starting points of the Clothoid cornering the first and subsequent offset lines respectively as shown in Figure 4.6. Let B be a point on the inner offset (second offset), normal to the Clothoid starting point A.

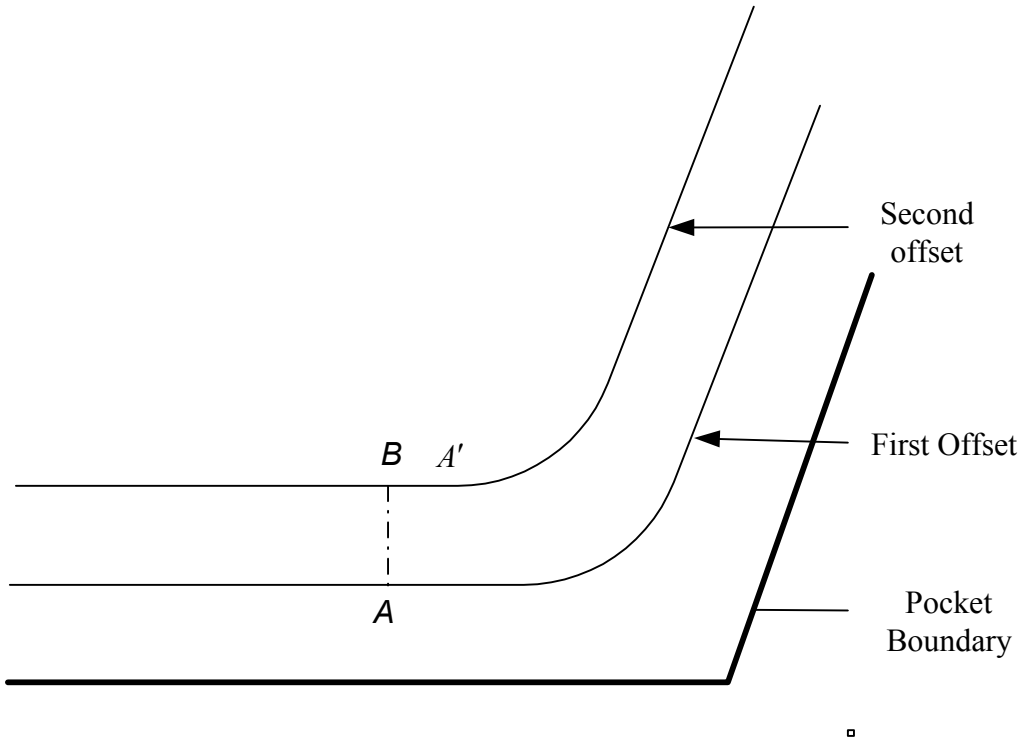

Figure 4.6 Clothoid start point search on second offset

A reasonable location for the Clothoid starting point A' is beyond point B on the inner offset. Any Clothoid starting before B will leave some uncut region between the first offset and the subsequent offset of the type *'second uncut region'* shown in Figure 4.5

Consider an arbitrary location for A' on the subsequent offset beyond B as shown in Figure 4.6. Let R be the perpendicular distance between the first and the second offsets. As we proceed along the Clothoid starting from A', the distance between the two offsets gradually reduces to a value below R (distance between parallel offsets) along the length of the Clothoid up to a certain point M shown in Figure 4.7. This is due to the fact

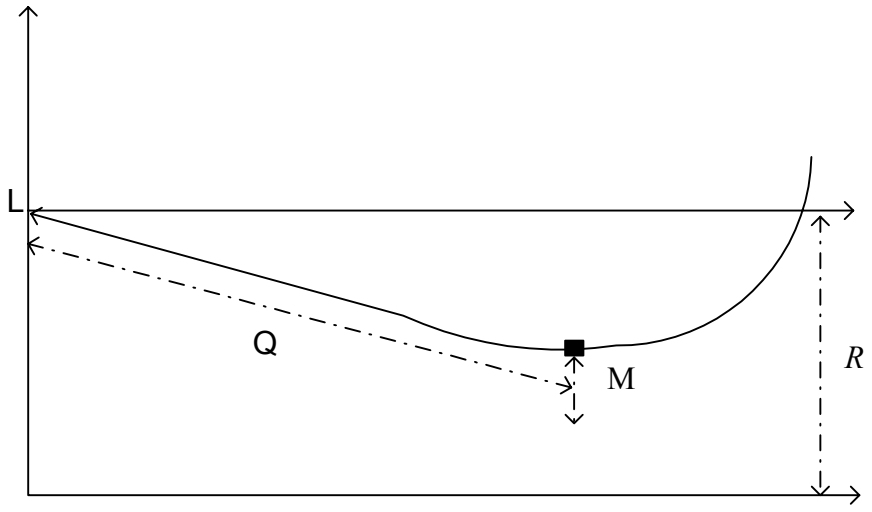

Figure 4.7 Curve showing the change in the distance between the Clothoids at the corners.

that the Clothoid starting point A' lies beyond point *B,* hence, there is a certain delay in the curvature of second offset Clothoid starting from A' as compared to the outer offset Clothoid starting from *A*.

Now since the curvature of the Clothoid on the second offset is greater then the curvature of the Clothoid on the first offset, because of the smaller scaling factor, the higher curvature of the Clothoid on the second offset (starting from point A') overrides the initial delay factor as we proceed further along the length of the first offset Clothoid corresponding to the curve beyond point *M* in Figure 4.7 thereby gradually increasing the distance between the two Clothoids of the offsets to a value more then *R*.

Therefore the starting point for the Clothoid for an inner offset should lie at some distance away from the corner such that the connecting point between two symmetrical Clothoids corresponds to some point on curve section Q in Figure 4.7.

But a point very close to L on curve part Q in figure (4) means that the starting point A' is too close to the corner of the second offsets resulting in a very small radius of curvature at the corner which will cause a jerk effect on the machine tool. It is therefore obvious that the starting point A' should lie at such a location which will result in the longest possible curve part Q in Figure 4.7 and A' corresponds to point M in Figure 4.7.

4.4 Proposed Clothoid Curve Tool Path Generation Algorithm

Based on the discussions provided in this chapter we now propose a Clothoid curve tool path generation algorithm that uses the Bi-Clothoids to obtain a smooth, continuous cornered boundary offset tool path for polygonal pockets.

Clothoid Curve Tool Path Generation Algorithm

Input

Polygonal Pocket Geometry

Cutting tool diameter, *d*

Initial Scaling Factor (Default Scaling Factor is 1)

Output

Boundary Parallel Offset tool paths

Start

Step 1. Calculate the slopes and angles formed by all the sides of the polygon

Step 2. Generate first boundary parallel offset polygon with a step distance of *d*/2

Step 3. Generate subsequent successive boundary offsets with step distance, *d*

Step 4. Calculate the starting point of the Clothoids at each corner of the first offset polygon.

Typically the distance for starting point of this Clothoid =*2*d.* It is also affected by the machine tool specifications and the amount of corner left over material that will be removed in the finishing operations.

Step 5. Calculate the value of the maximum parameter, $u_{\max}$ for all of the corners on the first boundary offset using Equation 3.12

The value of the $u_{\max}$ remains the same for the entire subsequent boundary offsets.

Step 6. Select any corner on the first boundary offset and calculate the symmetric Clothoids with an initial scaling factor, *a*= 1.

Step 7. Check if the symmetric Clothoids meet, if yes, proceed to Step 8, else proceed to Step 7.1

Step 7.1 Increase the scaling factor if the symmetric Clothoids cross each other or decrease the scaling factor if the symmetric Clothoids are short of meeting each other.

Step 7.2 Recalculate the Clothoids and repeat Step 7 until the symmetric Clothoids meet.

Step 8. Repeat Step 6 for all the corners of the boundary offset.

Step 9. Search for Clothoid starting point on the second boundary offset point.

Step 9.1 Select a corner of the second boundary offset

Step 9.2 Initial Clothoid starting point for the respective corner is a point on the second boundary offset that is normal to the starting point of the Clothoid on the first boundary offset

Step 9.3 Calculate the symmetric Clothoids

Step 9.4 Check if the symmetric Clothoids meet, if yes, proceed to step 10, else, change the parameter as explained in Step 7.1 and repeat the process from Step 9.3.

Step 10 Verify for any islands of the type second uncut region shown in Figure 4.4 and explained in Case 4.3.2. If there is no island proceed to Step 11, else, proceed to Step 10.1

Step 10.1 As explained in Case 4.3.2, move the starting point further towards the corner of the second boundary offset and repeat the process from Step 9.3

Step 11. Select the next corner of the second boundary offset and repeat the procedure starting from Step 9.2 until the Clothoids for all the corners of the second boundary offset are calculated.

Step 12. Consider the next boundary offset (third boundary offset) and let,

First boundary offset = Second boundary offset,

Second boundary offset = Third boundary offset.

Repeat the procedure starting from step 9.

Step 13. Repeat the Steps 9 to 12 until the corner Clothoids for all the boundary offsets have been calculated.

Step 14. Plot the offsets with the continuous corners formed by Clothoids.

End

The above presented algorithm can be used to generate smooth Clothoid curve tool paths for 2.5D high speed milling of polygonal pockets. With the smooth curvature transition at the corners formed by the Bi-Clothoids, the generated tool paths can be used for high speed machining with lesser acceleration variation of the cutter and the resultant high cutting impact to the cutters.

Chapter 5. COMPUTER IMPLEMENTATION AND EXAMPLES

In this chapter, the computer implementation of the proposed boundary offset tool path generation algorithm using Clothoidal curves is demonstrated. A step-by-step explanation of the tool path generation process is explained along with some computer-generated images of the tool path.

5.1 Computer Implementation

The proposed algorithm was implemented in MATLAB Version 6.5 programming tool. The program was run on a 1.63 GHz personal computer.

For a concave pocket example we considered polygonal pocket geometry of five sides shown in Figure 5.1. The tool path was generated using a cutting tool of radius 0.25 inches.

The traditional boundary offset spiral tool path for this kind of pocket in Figure 5.1 is shown in Figure 5.2. It can be clearly seen in the traditional tool paths that the corners make extremely sharp turns. As the cutting tool moves into these sharp corners, the acceleration of machine has to be instantly reduced resulting in a jerk motion effect on the machine tool. The radial depth of cut and chip sizes increase rapidly at the sharp corners. The cutting force and material removal rate is also very high in these areas which tend to reduce the productive life of the cutter and the machine tool. We expect our method of corner smoothing with the help of Clothoidal spirals will reduce all the above said problems by a considerable amount.

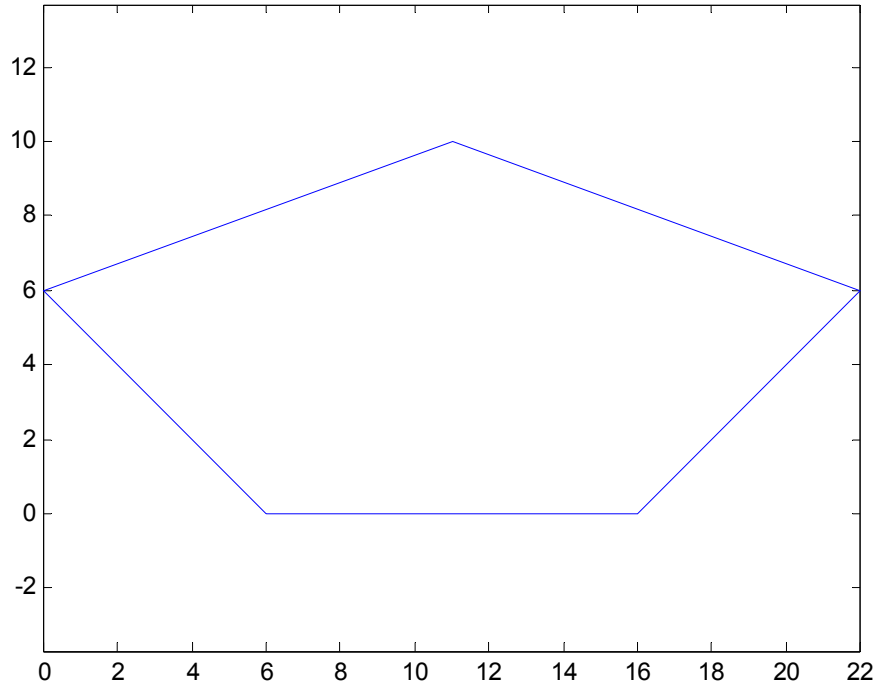

Figure 5.1 A five sided concave polygonal pocket

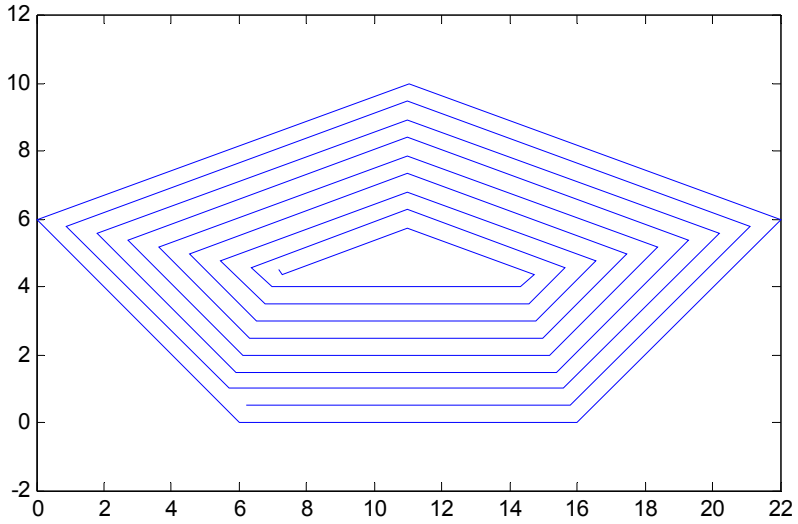

Fig 5.2 Traditional boundary parallel spiral tool path for concave polygonal pocket.

For our discussion we will consider only one corner of the polygonal pocket to demonstrate how the tool path was generated. The same process can be repeated for each of the corners to obtain the complete tool path. The maximum parameter, *u,* for the given dimensions of the pocket was calculated to be equal to 0.5.

For High Speed Machining it is important to use the full tool diameter for the width of cut in pocketing. Any smaller width of cut will strain the tool, because width of cut will increase as the tool enters a corner as shown in Figure 5.3. For example, a half-width cut becomes a full-width cut in the corner. Therefore An offset distance of 0.5*d, where d is the diameter of the cutting tool, was taken for the first offset.

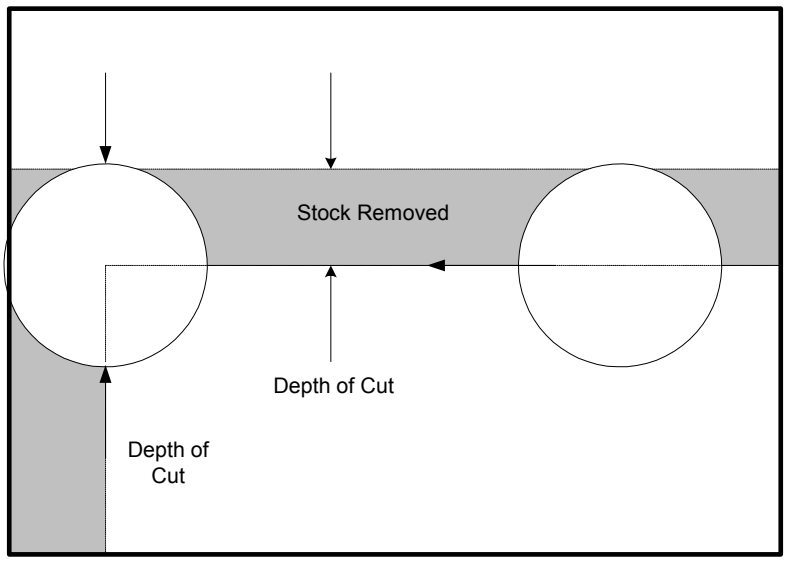

Figure 5.3 Half width cut becoming a full width cut in the corner.

The offset distance for the subsequent offsets is taken as diameter d. The starting point for the pair of Bi-Clothoids which is user defined as taken at a distance of 2*d on the offset lines from the corner. The first offsets along with the initial Bi-Clothoids for an initial scaling factor of a=1, is shown in Figure 5.4.

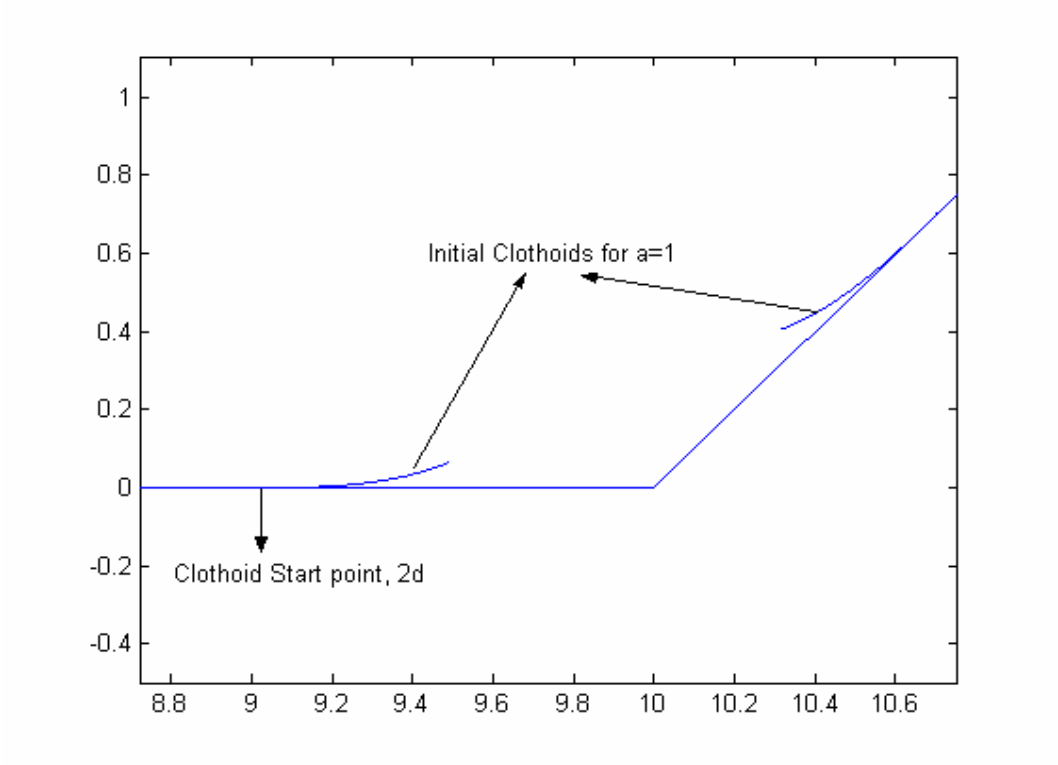

Figure 5.4. First offset and Clothoid start points with initial clothoids.

Since the two initial Clothoids do no meet each other the scaling factor is gradually increased until the Clothoids just meet at the ends. . If the initial Clothoids over cross each other, the scaling factor is gradually decreased till they just meet at the ends. The behavior of the initial clothoid with the gradual increase in scale factor is shown in Figure 5.5. Note that when the scaling factor is increased the curvature of the clothoids is decreased. This can also be seen in equation for curvature of the Clothoids,

$$c_v = \frac{\pi u}{a} \tag{5.1}$$

where scaling factor a is in denominator, thereby increasing the curvature, c_v every time the scaling factor is decreased.

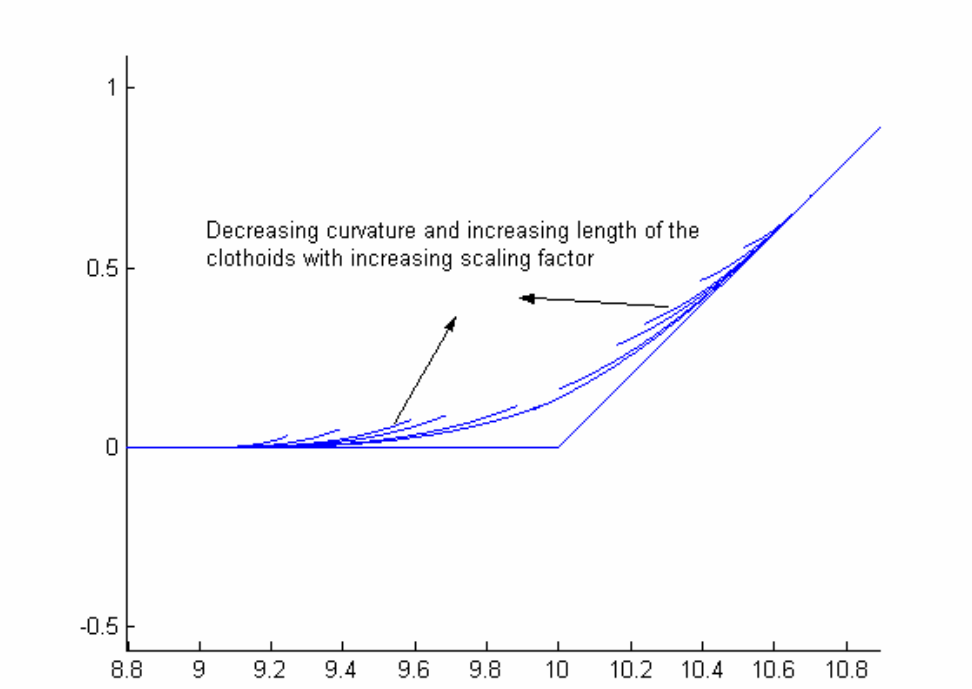

Figure 5.5. Changing the scaling factor to connect the Clothoids

In Figure 5.7, the second boundary offset is shown along with the Bi-Clothoids at the corner. Initial starting points for the Bi-Clothoids were the points lying on the second offset which are normal to the starting points on the first offset. The Bi-Clothoids starting from the initial starting points tend to leave some uncut region. This is because the Clothoids on the second offsets have higher curvature due to lower scaling factor. The upward curl of the Clothoids on the second boundary offsets is faster then the upward

curl of the Clothoids on the first boundary offsets. As a result the distance between the uncut Clothoids of first boundary offset lines and the Clothoids of the second boundary offset lines is more at the tips of the Clothoids as compared to the start point of the Clothoids.

To avoid this kind of uncut region the Clothoids have to be moved further near to the corner as explained in the previous chapter. An example indicating the behavior of the Bi-Clothoid as it's starting point is moved nearer to the corner is show in Figure 5.5 In Figure 5.7 this is shown by another Clothoid on the second boundary offset which is slightly nearer to the corner as compared to the initial Clothoid that was plotted on the second boundary offsets. This new Clothoid is also tested for any uncut regions. The testing is done by measuring the distance between the connecting point of the Bi-Clothoids on the second boundary offsets and the connecting point on of the Bi-Clothoids on the first boundary offsets. As discussed in the previous chapter the distance between these Bi-Clothoid connecting points tends to be the maximum. If this maximum distance is lesser then or equal to the offset distance d, then it indicates that there is no uncut region in that corner and therefore the current pair of Bi-Clothoids can be accepted as the tool paths cornering the current boundary offset lines. Similarly Bi-Clothoids are calculated for all the corners for the current offset as well as the subsequent offsets.

Figure 5.8 shows the contour parallel spiral tool path for the polygonal pocket shown in Figure 5.1 developed using the proposed algorithm. The entire boundary parallel offset sharp edge corners have been replaced with bi-clothoids resulting in

smooth continuous corners. Figure 5.9 shows another example of smooth cornered tool path for a polygon.

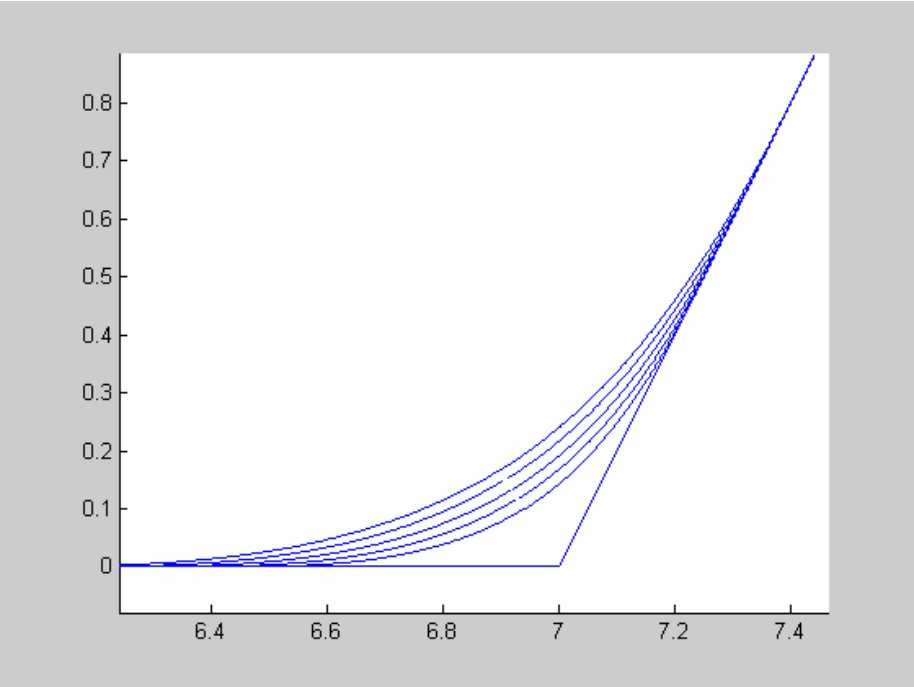

Figure 5.6 Increasing curvature of the Clothoid as the starting point is moved nearer to the corner of the offsets.

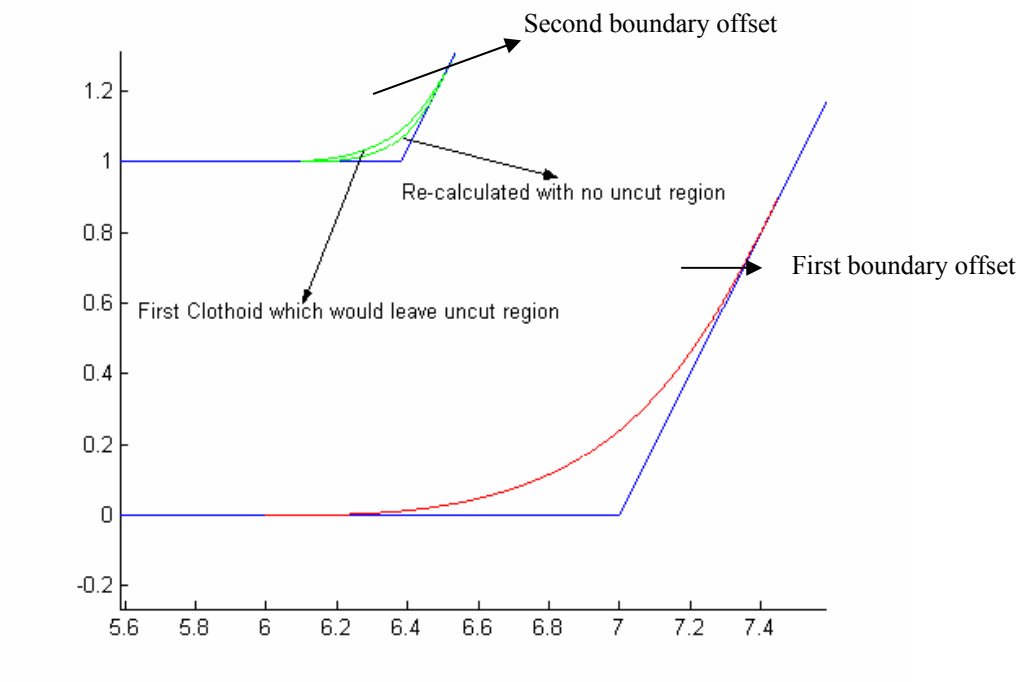

Figure 5.7. Bi-Clothoids for the second boundary offsets.

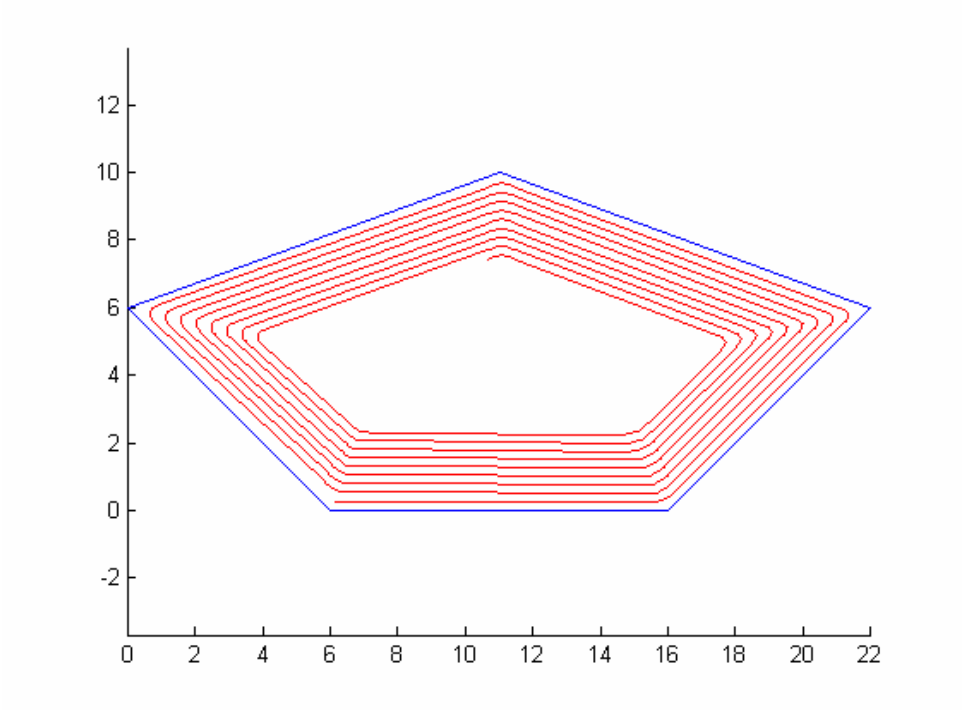

Figure 5.8 The spiral tool path with smooth corners

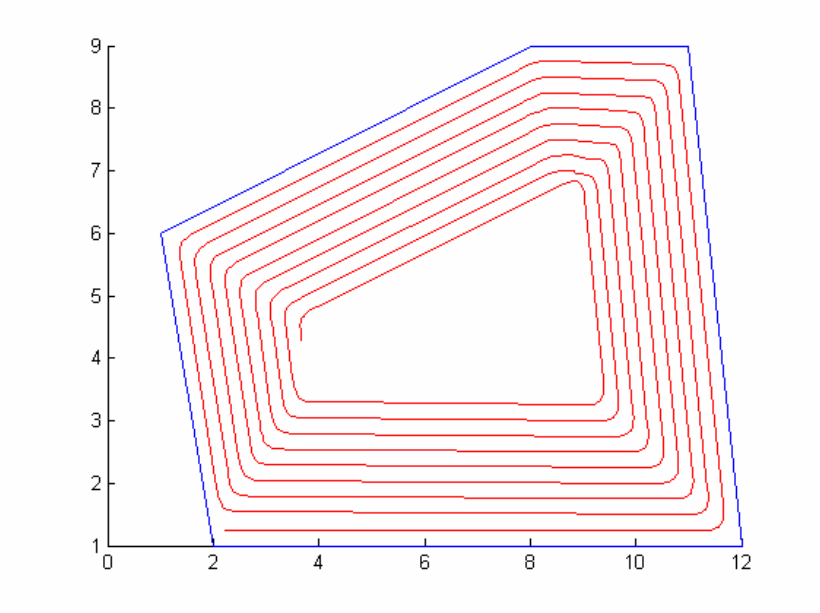

Figure 5.9 Another example of spiral tool path with smooth corners

5.2 Summary

In this chapter the implementation of our proposed algorithm for using Clothoidal splines (Bi-Chlothoids) for contour parallel tool path cornering was demonstrated. Tool path by the proposed method for an example part has also been presented. The important steps in the execution of the algorithm were discussed.

Chapter 6. CONCLUSION

6.1 Conclusion

In this paper a new and non conventional method to generate contour parallel offset tool paths for 2.5D pocket milling has been introduced. We have used the Clothoidal curves which have traditionally been used in the Highways and Rail tracks construction to replace the sharp corners in 2.5D polygonal pockets.

The proposed algorithm to generate the new type of tool path has been discussed. The algorithm presented does not leave any uncut regions in between the contour parallel offset tool paths. The algorithm uses an iterative method to determine suitable symmetric Bi-clothoids to make sure that no uncut regions are left behind in the interior of the pocket. To reduce the number of iterations needed to determine the right Clothoids a start point of search was identified based on certain logical observations.

The proposed algorithm was programmed and run on example polygonal pockets to generate a spiral tool path. The resultant corners are smooth and continuous in nature. The unique property of the linear curvature variation along the length of curves will be extremely useful for high speed motion of the cutting tool along the corners of these pockets. The smooth Clothoidal Corners are intended to result in smoother machine tool acceleration and deceleration at the corners as compared to conventional Circular Arc Corners. The stresses and forces induced on the cutter and the machine tool spindle will be comparatively reduced due to the linear curvature variation of the Clothoids at the

corner resulting in longer cutting tool and machine tool, life. Better acceleration at the corners will also help in reducing the overall cycle times of machining.

6.2 Future Work

The proposed method can be further extended for pockets of more complex boundaries, pockets with islands, etc. Methods for connecting other geometric curves such as a circle with a circle or a line with a circle have already been published been published by [Meek and Walton, 1989] giving us an opportunity to try more complicated pocket geometries. There is also a lot of scope to combine this method of tool path generation with online federate optimization to take maximum use of the capabilities of the available high speed machine technology.

The proposed method may also be useful in Robots for painting and welding applications whose motion paths are planned on similar concepts.

References

1. Bae S, Ko K, Kim B, Choi B, "Automatic federate adjustment for pocket milling", Computer-Aided Design vol.35, (2003), 495-500.
2. Bieterman M and Sandstrom D, "A curvilinear tool-path method for pocket machining", Proceedings of IMECE 2002, ASME, Nov 17-22, 2002, New Orleans, Louisiana, USA.
3. Boersma J, "Computation of Fresnel Integrals," Math. Comp, vol. 14, (1960), p. 380.
4. Chan K W and Choy H S, "A corner looping based tool path for pocket milling", Computer Aided Design, vol.35, (2001), 155-166.
5. Choi B K and Kim B H, "Die Cavity pocketing via cutting simulation", Computer Aided Design, vol.29, no.12, (1997), 837-846.
6. Choi B K and Kim B H, "Machining efficiency Comparison, Direction parallel with contour parallel tool path", Computer Aided Design, vol.34, (2002), 89-95.
7. Choi B K and Park S C, "A pair-wise offset algorithm for 2D point-sequence curve," Computer Aided Design, vol.31, no.12, (1999), 735-745.
8. Choi B K and Park S C, "Uncut-free pocketing tool paths generation using pair-wise offset algorithm," Computer Aided Design, vol.33, no.10, (2001), 739-746.
9. Cody W J, "Chebysev approximation for the Fresnel Integrals," Math. Comp, vol. 22, (1968), 450-453
10. Dagiloke I, Kaldos A, Douglas S, Mills B, "High speed machining: an approach to process analysis", Journal of Materials Processing Technology, 54, (1995), 82-87.

11. Dey T, Zhao W, “Approximate medial axis as a Voronoi sub complex”, Computer-Aided Design, (2003)
12. Fallbohmer P, Altan T, Tonshoff H, Nakagawa T, “Survey of the die and mold manufacturing industry’, Journal of Materials Processing Technology, vol. 59, (1996), 159-168
13. Farouki R, Tsai Y, Wilson C, “Physical constraints on federates and feed accelerations along curved tool paths”, Computer-Aided Design vol.75, (2000), 337-359.
14. Flutter A, Todd J, “A machining strategy for tool making”, Computer-Aided Design vol.33, (2001), 1009-1022.
15. Gray A, Modern Differential Geometry of Curves and Surfaces with Mathematica, Second Edition, (1997), 64-66.
16. Hansen A and Arbab F, “An algorithm for generation of NC tool paths for arbitrarily shaped pockets with islands”, ACM Trans Graph , Vol.11, No.2,(1992), 152-158.
17. Hastings C, Jr, “Approximations for calculating Fresnel Integrals,” Math. Comp. [MTAC], vol. 10, (1956), p. 173.
18. Hatna A, Grieve R, Broomhead P, “Automatic CNC milling of pockets: geometric and technological issues”, Comp. Intergraded Manufacturing Systems, vol.11, No. 4, (1998), 309-330.
19. Heald M, “Rational Approximations for Fresnel Integrals,” Math. Comp, vol. 44, (1985), 459-461.

20. Heald M, “Rational Approximations for the Fresnel Integrals”, Mathematics of Computation, Vol.44, Issue 170 (1985), 459-461.
21. Held M, “Voronoi Diagrams and offset curves of curvilinear polygons”, Computer-Aided Design vol.30,no.4, (1998), 287-300.
22. Held M, Lukacs G, Andor L, “Pocket machining based on contour –parallel tool paths generated by means of proximity maps”, Computer-Aided Design vol.26,no.3, (1994), 189-203.
23. Held M, “VRONI: An engineering approach to the reliable and efficient computation of the Voronoi diagrams of points and line segments”, Computational Geometry, vol.18, (2001), 95-123.
24. Ibaraki S, Ogawa T, Matsubara A, Kakino Y, “Model based learning of cutting forces in end milling processes”, Japan-USA Symposium of Flexible Automation, (2002)
25. Jayaram S, Kapoor S, DeVor R, “Estimation of the specific cutting pressures for mechanistic cutting force models”, International Journal of Machine Tools and Manufacture, vol. 41, (2001), 265-281.
26. Kakino Y, Saraie H, Ohtsuka H, Nakagawa H, “Intelligent end milling system and its application to internal cylindrical machining with spiral curves”, Japan-USA Symposium of Flexible Automation, (2002)
27. Klaus D M, “Computation of Fresnel Integrals,” J. Res. Natl. Inst. Stand. Techno. vol.102, (1997), p. 363
28. Ko J, Yun W, Cho D, “Off-Line feed rate scheduling using virtual CNC based on an evaluation of cutting performance”, Computer-Aided Design, (2002).

29. Lee E, “Contour offset approach to spiral tool path generation with constant scallop height”, Computer-Aided Design vol.35, (2003), 511-518.
30. Makino H, “Clothoidal Interpolation – A New Tool for High-Speed Continuous Path Control”, Annals of CIRP, vol. 37, no. 1, (1988), 25-28.
31. Meek D S and Thomas R S D, "A guided clothoid spline", Computer Aided Geometric Design vol.8, (1991), 163-174.
32. Meek D S and Walton D J, "Offset curves of Clothoidal splines", Computer-Aided Design 22(1990), 199-201.
33. Meek D S and Walton D J, "The use of Cornu spirals in drawing planar curves of controlled curvature", Journal of Computational and Applied Mathematics 25,(1989), 69-78.
34. Narita H, Shirase K, Wakamatsu H, Tsumaya A and Arai E, “Autonomous milling process control based on real time cutting simulation”, Japan-USA Symposium of Flexible Automation, (2002)
35. Otsuka H, Yamazi I, Ito T, Ihara Y, Kakino Y, Matsubara A, “Advanced feed forward control for constant cutting forces in die machining”, Japan-USA Symposium of Flexible Automation, (2002)
36. Park S, “Tool-path generation for Z-constant contour machining”, Computer-Aided Design vol.35, (2003), 27-36.
37. Park S, Choi B, Chung Y, “Contour-parallel offset machining without tool-retractions”, Computer-Aided Design vol.35, (2003), 841-849.
38. Persson H., “NC machining of arbitrarily shaped pockets”, Computer Aided Design, vol.10,no. 3, (1978), 169-174.

39. Renton D, Elbestawi M A, " High speed servo control of multi axis machine tools", International Journal of Machine Tools and Manufacture, vol. 40, (2000), 539-559
40. Richards N, Fussel B, Jerard R, "Efficient NC machining using off-line optimized feedrates and on-line adaptive control", Symposium on Process Planning and Process Optimization, (2002), IMECE, New Orleans, 1-11.
41. Roth D, Ismail F, Bedi S, "Mechanistic modeling of the milling process using an adaptive depth buffer", Computer-Aided Design,vol.35, no.14, (2003), 1287-1303.
42. Stori J A and Wright P K, "A constant engagement offset for 2-1/2D tool path generation", Proceedings of the ASME, MED, vol.8, (1998), 475-481.
43. Tlusty J and Smith S, "Current trends in high speed machining", Transactions of ASME, vol.119, (1997), 664-666.
44. Walton D J and Meek D S, "Clothoidal splines", Computers and Graphics vol.14, (1990), 95-100.
45. Wang J, Ravani B, "Computer aided contouring operation for traveling wire electric discharge machining (EDM)", Computer-Aided Design vol.35, (2003), 925-934.
46. Wang L, Miura K, Nakmae E, Yamamoto T, Wang T, "An approximation approach of the clothoid curve defined in the interval [0, pi/2] and it's offset by free form curves", Computer-Aided Design, vol.33, (2001), 10419-1058.
47. www.mathworld.wolfram.com
48. www.mmsonline.com

49. Xu H, “Line and angular federate interpolation for planar implicit curves”, Computer-Aided Design vol.35, (2003), 301-317
50. Yong T, Narayanaswami R, “A Parametric interpolator with confined chord errors”, acceleration and deceleration for NC machining”, Computer-Aided Design, (2003).
51. Zhang L, Fhu J, Nee A, “Tool path regeneration for mold design modification”, Computer-Aided Design vol.35, (2003), 813-823.
52. Zhao M, Balchandran B, “Dynamics and stability of milling process”, Intl. J. Solids and Structures, 38, (2001), 2233-2248.